STUDIES OF IRON REMOVAL IN DRINKING WATER USING LIMESTONE AS ADSORBENT

BY

PHIRI THANDIWE

[ID #: 10586851]

THIS THESIS IS SUBMITTED TO THE DEPARTMENT OF MEDICAL PHYSICS
SCHOOL OF NUCLEAR AND ALLIED SCIENCES
UNIVERSITY OF GHANA, LEGON

IN PARTIAL FULFILMENT OF THE REQUIREMENTS FOR THE DEGREE OF
MASTER OF PHILOSOPHY

IN

NUCLEAR SCIENCE AND TECHNOLOGY

JULY, 2017

DECLARATION

I, **Phiri Thandiwe**, hereby declare that this thesis is a result of my research work undertaken as a student at the School of Nuclear and Allied Sciences, University of Ghana, under the supervision of **Dr. Dennis K Adotey** and **Prof. Samuel B. Dampare**. It contains no material previously published by another person for any other award. In the case where other sources of information have been used, such sources have been cited in this work and duly acknowledged under references.

…… … …..……..

PHIRI THANDIWE, ID: 10586851 DATE

Student

…… ...…...……..

DR. DENNIS K. ADOTEY DATE

Principal Supervisor

……. ….....……

PROF. SAMUEL B. DAMPARE DATE

Co-Supervisor

DEDICATION

I dedicate this work to everyone who is inspired by science

ACKNOWLEDGEMENT

I am very grateful to my supervisors, Dr. D. K. Adotey and Prof. S. B. Dampare for their guidance, constructive criticism and input in my work. Throughout my work, I also received support and assistance from a number of individuals and institutions to which I am very grateful. The institutions are; the International Atomic Energy Agency (IAEA) which awarded me scholarship for the whole program; The Dean, Administrators, Lecturers and staff of School of Nuclear and Allied Sciences (SNAS), The Ghana Atomic Energy Commission [Radiation Protection Institute, National Nuclear Research Institute (Accelerator Research Centre, and Nuclear Chemistry and Environmental Research Centre). The Department of Chemistry and Department of Earth Science, University of Ghana Main Campus. I also wish to acknowledge with sincere gratitude the support I received from my senior and junior colleagues at the Zambia National Institute for Scientific and Industrial Research (NISIR), Lusaka. I acknowledge the love, prayers, moral and social support from my family, Mr. Silas Chabi (for continuously helping and encouraging me every time I needed help), friends and the Church. Above all, I honour God Almighty for His Grace and Wisdom which have always been sufficient in my times of need.

ABSTRACT

The study assessed the suitability of two limestone samples (EKLD01 and EKLR02) for use as adsorbent to remove excess iron in drinking water through geochemical and mineralogical characterization using an ion beam linear accelerator and petrographic thin sectioning respectively. The radiological safety (activity concentration) of the limestone was evaluated through measurement of the Naturally-Occurring Radioactive Materials (NORMs) using a High-Purity Germanium (HPGe) γ-ray Semi-conductor Detector. In addition, the study monitored the iron adsorption efficiency (sorption capacity and percentage adsorption) of limestone with respect to Sample Size, Adsorbent Dose, Residence Time and pH. Agreement between the adsorption isotherms obtained from this study and model adsorption isotherms proposed by Langmuir (1916) and Freundlich (1909) assessed. The iron removal technique was developed using limestone grain sizes (500-1000 µm, 1000-2000 µm and 2000-6350 µm) through Batch Adsorption experiments using Iron standard solutions, followed by Column Adsorption experiments using iron rich/contaminated ground water from the Ashongman Estates, in the Ga East Municipal of the Greater Accra Region of Ghana. The geochemical and mineral characterization indicated that Sample EKLR02 was the most suitable limestone sample for the development of technique based on its relative high calcium content (56.14%). Radiologically, both limestone samples were safe as their calculated mean annual effective dose (0.2 mSv/yr for both samples) did not exceed the UNSCEAR (2000) recommended value of 0.4 mSv/yr. In the Batch experiment, the extent of iron adsorption with respect to time, pH, and dosage of limestone (20-100 g in 200 mL of iron standard solution) were studied. Maximum adsorption was attained at pH 12, limestone dosage of 100g/200 mL, time of 60 minutes, and particle size of 500-1000 µm. Consequently, these were adopted and used for the Column experiments.

In the Column experiments, optimal conditions obtained during the Batch experiments were adapted and used to analyze fourteen (14) water samples from boreholes and hand-dug wells from the Ashongman Estates. The measured iron concentrations of the sampled water from Ashongman Estates ranged from 0.20 to 4.66 mg/L prior to the Column experiment. At the end of the Column experiment, the measured iron concentrations ranged from 0.19 to 0.28 mg/L [below the World Health Organization (WHO) recommended level of 0.3 mg/L]. There was linear agreement (R_L =1) between the adsorption data obtained from the study with Langmuir's Model Adsorption Isotherm (1916) at iron concentrations of 1 mg/L and above (in the ground water samples). The adsorption data obtained from the study did not correlate well (R^2 = 0.0138) with the Freundlich model adsorption isotherm (1909); and the Freundlich constant, K_f , was found to be negative -5.2367 instead of a positive value.

TABLE OF CONTENTS

LIST OF TABLES

LIST OF FIGURES

ABREVIATIONS

A	Absorbance
CCBM	Calcium carbonate-based materials
C	Solution equilibrium concentration
C_m	Molar concentration of solute
C_e	Equilibrium concentration of adsorbate (mg/L)
C_o	The highest initial adsorbate concentration (mg/L)
E	Molar absorptivity
Fe	Iron
I_0	Intensity of light incident upon sample cell
I	Intensity of light leaving sample cell
K_f	Freundlich constant
K_L	Langmuir adsorption constant (L/mg).
L	length of sample cell (cm)
m	Mass of adsorbent
n	Freundlich constant.
Q_e	Amount of adsorbate adsorbed at equilibrium (mg/g)
Q_{max}	Maximum monolayer adsorption capacity of the adsorbent
R_L	Langmuir separation factor or equilibrium parameter
w	Mass of solute adsorbed

CHAPTER ONE

INTRODUCTION

1.1 Background

Ground water, found in aquifers below the surface of the earth, is an important natural resource in the world. It is mainly as a result of rain water that falls onto the ground and seeps below the earth's surface through the crevices, joints, soil and fissures that accumulates and is known as ground water. It is the source of over 40% of the water that humans use both for public and domestic worldwide. Ground water accounts for 90% of water drunk in rural areas in which it is difficult for sewage companies to provide. Approximately 42% of water from the ground is used for irrigation purposes and it sustains vegetation on land. It is usually a permanent source of water as the rate of evaporation underground is minimum (Glynn, 2005).

Underground water is usually accessed through boreholes and wells, but it may reappear as springs, along joints or fissures. Iron is a natural mineral present in nearly every water supply, it is normally found as a divalent ion (Fe^{2+}), Rural ground water supplies usually have excess iron as a common problem, it usually has a concentration levels ranging from 0 to 55mg/L (Jusoh et al., 2005). While WHO recommended levels are below 0.3 mg/L Iron levels, above the WHO recommendation creates serious aesthetic problems (WHO, 1996).

Iron is found in the aquifer naturally, but it also be increased due to weathering iron bearing rocks, sewage and landfill leachate also dissolution of ferrous borehole and hand pump components (contamination) [Egboka,1989].

Iron has beneficial and adverse effects, minimal amounts of iron in water add to the alkalinity of water to make it tastier, easy to digest and nutritious. Nevertheless excess iron in water results in undesired effects such as brown stains on appliances (Fig 1.1), sinks, toilets plus bathtubs. Excess iron in humans can lead to death from extensive gastrointestinal hemorrhage. It can cause food and water to be discolored and develop a metallic taste (WHO, 1996).

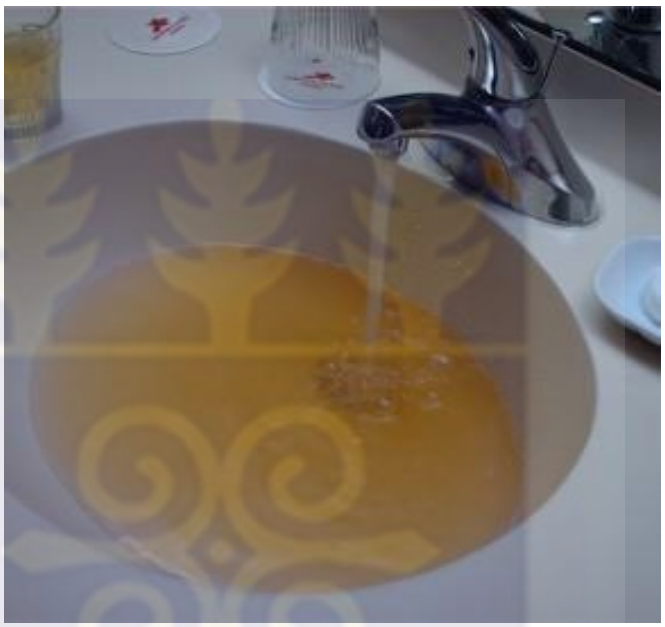

Fig 1.1: Iron water flowing from tap

To remove excess levels of iron in water there is need for development of water purifying techniques. There are some effective solutions to this problem. A standard water softener and reverse osmosis systems will efficiently remove iron from water in most cases, however it is costly and rural dwellers cannot afford. The use of permeable membranes, Ion exchange, Oxidation and Microfiltration are also very well-known methods of iron removal despite usually taking up time and expensive cost. These methods are however not as effective as reverse osmosis (Gupta et al., 2005).

Another common method used is adsorption (Devi, 2013). This method is user friendly and is preferred because it is inexpensive; and iron is known to adsorb onto surfaces of

substances by creating complex compounds with the surface of materials, some of these materials being CCBM (calcium carbonate-based materials) [Gupta et al., 2005].

One readily available and cost effective CCBM is limestone; known to form various compounds with elements in nature. Although limestone has been used in water purification, its use has not been well exploited in Ghana and Zambia .The main emphasis in the use of limestone has been on pH adjustment. It is used to raise the pH of water and act as a neutralizing agent in acidic water: it also helps in corrosion control. Addition of limestone to water causes oxidation of Iron to produce Siderite and $CaFe(CO_3)_2$ as the main products of the reaction. Limestone is crushed and slacked with water to produce slacked lime [$Ca(OH)_2$] known as Lime Softening and is the major use of limestone in water purification. This produces large values of a mixture of $CaCO_3$ and $Mg(OH)_2$ [calcium carbonate and magnesium hydroxide] in a very finely divided white precipitate,with a large surface area. Limestone can easily have substances adsorb to it as compared to most compounds, and can be used in the adsorption process to remove excess iron in water (Mook, 2000). A technique will be developed in Ghana which will then be applied in Zambia.

1.2 Application of Cost Effective Adsorption Technique for Removal of Iron in Zambia

Mongu (15˚16’39”S 23˚7’55”E) formerly known as Barotse land, the provincial headquaters of Western Province Zambia, Mongu is located 610 km North-West of Lusaka the Capital city of Zambia (about about 6-8 hour drive). With a population of 179,585 people from the last census conducted in 2010 (Census Report., 2010). It is well-known for carpet and basket weaving and is the major rice growing region in Zambia

Fig 1.2: Map of Zambia showing location of Mongu and Lusaka (Capital of Zambia)

There are three eco-regions in Mongu, flood plains which are flooded by the Zambezi River, the higher dry ground and the cryptosepalum dry forests. The area is sandy and flat with land being dry most times. Many regions do not have surface water and people solely depend on underground water.

Mongu has for many years been known to have poor water supply for its residents, the water is known to be iron rich and emerges out of taps with a brownish color with an unpleasant odor. The presence of iron in water is mainly attributed to corroding of iron containing mineral deposits and rocks, industrial effluent, acid-mine drainage, sewage as well as landfill leachate (Osborne, 2000).Various attempts such as the use of filters, reverse osmosis and oxidation to mention a few have been made to reduce the iron in

water by (WWSC) Western water and Sewerage Company, but over the years have proven to be too expensive or unsuccessful leading to frustrations. Due to the dryness of Mongu, Boreholes have been dug by the locals to have water easily as stated that some regions do not have any surface water but the geographic region has a lot of iron in the rock and iron has been found in the boreholes too (Osborne,2000).

1.3 Research Problem

Excess levels of iron present in ground water results in aesthetic problems such as Brownish-red colour of water with an unpleasant odour. It results in stains on laundry, dishes, tubes and sinks. Iron in water results in rusting of water pipes which in turn causes clogging of water pipes. Due to the health implications of Iron in the human body, there is a need to remove residual Iron in drinking water. There several of methods that are used to remove iron from water; however these methods have limitations and are usually not as effective and setup are usually costly, accordingly, there is the need for the development of cost effective Iron removal technique to help solve the problem.

- Photographs showing the effects of high iron contents in water. (Fig 1.3 a and b)

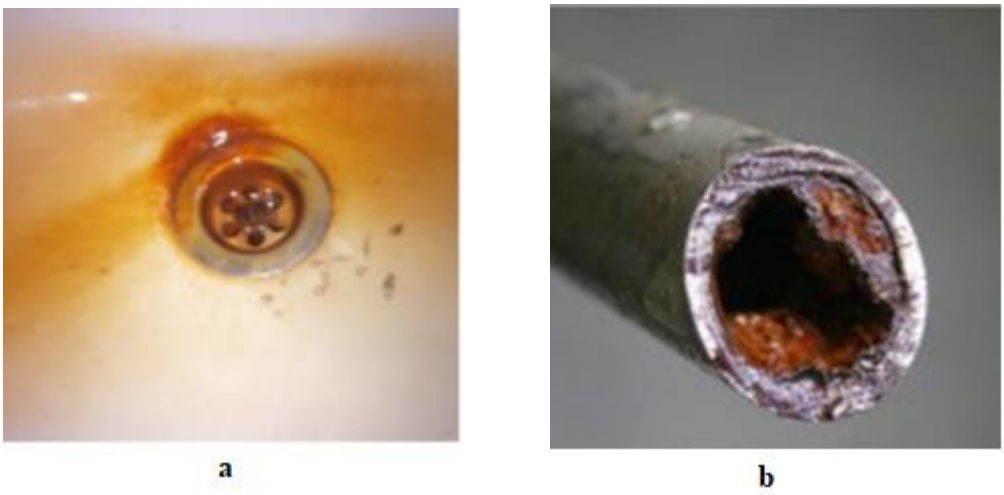

Fig 1.3: (a) Sink stained with Iron; (b) Clogged pipe due to accumulation of Iron

1.4 Research Objectives

1.4.1 Core Objective

To assess the suitability of limestone as an adsorbent for the removal of excess iron in drinking water.

1.4.2 Specific Objectives

a) To remove excess iron from drinking water using limestone as adsorbent;

b) To characterize limestone geochemically and mineralogical;

c) To assess the radiological risk and safety associated with the use of limestone as adsorbent for the removal of iron in water. (Activity concentration and annual effective dose using a gamma detector.);

d) To assess the iron adsorption efficiency (sorption capacity and percentage adsorption) of limestone with respect to varying:

   i) adsorbent dose

ii) particle size of the adsorbent (limestone)

iii) residence time

iv) pH; and,

e) To compare the adsorption data (results) with model adsorption isotherms by Langmuir (1916) and Freundlich (1909); and to show the relationship between the equilibrium concentrations of iron adsorbed with its mass onto limestone adsorbent.

CHAPTER TWO

LITERATURE REVIEW

This chapter provides information about Iron, adsorption, gamma spectroscopy, UV spectroscopy, limestone and accelerators as stipulated in various texts

2.1 Water

Water is considered not merely the medium of life, nonetheless it is fundamental and plays a pivotal role when it comes to sustainable economic growth of a nation. Ground water is one of the primary sources of fresh, clean water aimed at sustaining life. Unfortunately, irrigation processes in the agriculture sector and industrial applications are some of the main applications that are increasingly depleting ground water. In addition, contamination with various pollutants as well as other uses are also contributing to ground water depletion. Urban areas are more likely to have access to safe drinking water as compared to rural areas with about 91% and 69% respectively (Kriš et al., 2005). Rural areas are prone to unsafe water.

Problems dealing with water not only affect humans but the environment at large which includes plants and animals.

2.2 Iron

It has the symbol **Fe** and its atomic number is 26.iron is found in the transition series, with a mass that makes it the most common element found in the world it is found naturally occurring, and forms most of Earth's external and internal core. It (iron) is found rarely on the surface of the Earth because it usually oxidizes, its oxides are pervasive and represent the primary ores. The internal core is believed to consist largely of an iron-nickel alloy; which is about 35% of the earth’s mass.

A large part of iron present in the earth's crust, are compounds hematite (Fe_2O_3), magnetite (Fe_3O_4), and siderite ($FeCO_3$) made with oxygen. Various igneous rocks are made up of iron sulfide minerals called pyrrhotite and pentlandite .

Excessive iron metal and Iron particles in water provisions cause several known problems. These include bad sense of taste, staining, deposition and suspension in the circulation system., which lead to problems such as stained teeth and brown colour stained toilet wares just to mention a few. It is the main cause for staining of iron-rich drinking water distribution systems. (Postawa et al., 2013)

Common adverse health effects of iron include breakdown of vital organs such as kidneys, liver and cerebral system. Iron is a metal that is useful in the human body but too much iron can cause disorders, hemochromatosis as it is known can lead to death. Several people are genetically vulnerable to excess iron. Overloads of iron ingestion causes excessive heights of free iron in the blood and high blood levels of free ferrous iron react with peroxides to produce highly reactive free radicals that can damage DNA, proteins, lipids, and other cellular components. This is known as Iron toxicity thus when the cell contains free iron, due to iron levels exceeding the recommended amount.

Iron is usually removed in groundwater management, nevertheless, the iron removal is usually unfinished. Various methods for removing iron are known but they have limitations.

2.2.1 Oxidation / filtration and iron Exchange.

2.2.1.1 Ion Exchange

Ion exchange is considered only for the removal of minor amounts of iron and manganese. It consist of the use of synthetic resins where an ion on the solid phase (the "adsorbent," usually sodium) is replaced for the unwanted ions in the water. Some of

the major problems in using this process for adjusting iron and manganese is that if some oxidation occurs during the process, the subsequent precipitate can coat and foul the media. Concentration of iron beyond 5 or 6 mg/L, dissolved in the water, require different methods. (Iron in drinking water, Montana Department of Quality, 2011).

2.2.1.2 Oxidation- Filtration

Oxidation is coupled with filtration. The oxidant oxidizes the iron or manganese while the filter then removes the iron particles.

Before filtration, there is need for oxidation to a state in which the ions can form insoluble complexes to occur. During Oxidation there is transfer of electrons from the iron and manganese being treated to the oxidizing agent. There two types of Oxidation

2.2.1.3 Ozonation

Usually ozone generators are used to create ozone which is fed by a pump into the water stream to change iron into ferric iron. This is followed by a contact time tank and then it is passed through a catalytic medium or an inert multilayered filter for elimination of the ferric iron (Iron in drinking water, Montana Department of Quality, 2011).

2.2.2.4 Clhlorination

Chlorine can be added into water as a gas; as calcium hypochlorite; or as sodium hypochlorite. Treated water is held in a withholding tank in which the iron precipitates out or flocculates into large enough particles that are then removed by filtration with manganese greensand, anthracite/greensand, or activated carbon (Iron in drinking water, Montana Department of Quality, 2011).

2.2.1.5 Aeration

In this process air is also used to turn dissolved iron into a substance that can be filtered. In a two tank system, air is introduced into the first tank using a pump or other injection device. The dissolved iron precipitates in the first tank and is carried into the second tank where it is filtered in a Birm or multi-media filter. One disadvantage to this system is that water bearing the precipitated iron goes through the head of the first unit and the piping between the units. At lower flow rates, the sticky ferrous hydroxide tends to foul the valve on the first unit. A single-tank system essentially combines the two tank system into a single tank system. The iron is oxidized at the top of the tank before falling into the filter medium at the bottom. There is no potential fouling of the head. Iron is filtered before it goes through the exit port of the valve (Iron in drinking water, Montana Department of Quality, 2011).

2.2.1.6 Oxidizing Separation

One of the most common chemical oxidant used is Manganese Greensand. It is very effective in the removal of iron. It is chiefly made up of the mineral glauconite which is granular. The material has a manganese oxide coat surrounding it (Iron in drinking water, Montana Department of Quality, 2011).

Removal of iron from groundwater is a collective treatment step in the production of drinking water nevertheless the water quality in the distribution system can depreciate due to settling of iron (hydroxide) particles or post-treatment flocculation of dissolved iron. Therefore, it is important to remove dissolved and particulate iron (Iron in drinking water, Montana Department of Quality, 2011). The adsorption technique has consistently been found to be economical and suitable for developing countries because of its treatment and cost efficiency.

2.3 Adsorption

Adsorption is the adhesion of atoms, ions or molecules from a gas, liquid or dissolved solid to a surface. The process makes a film of the adsorbate (material being adsorbed) on the surface of the adsorbent. It is different from absorption in which the adsorbate is dissolved by or permeates a liquid or solid (the absorbent). Adsorption is a surface-based process while absorption involves the whole volume of the material. The term sorption encompasses both processes.

Adsorption occurs in many systems and is extensively used. Atoms or molecules of a solid surface behave like the surface molecules of a liquid. These are not surrounded by atoms or molecules of their kind. Therefore, they have unbalanced or residual attractive forces on the surface which can hold adsorbate particles. The adsorbed atoms or molecules can be held on the surface of a metal such as platinum (Pt) by physical van der Waal's force or chemical forces due to residual valence bonds (Peköz, 2012).

2.3.1 Types of adsorption

The adsorption onto a solid surface is mainly of two types:

(*a*) **Physical Adsorption**

This is due to molecules being held to the solid surface by van der Waal's attractive forces. It is also referred to as van der Waal's Adsorption. For example, adsorption of hydrogen or oxygen on charcoal is Physical Adsorption.

(*b*) **Chemical Adsorption or Chemisorption**

In this kind of adsorption, molecules are attached to the solid surface through chemical bonds. These bonds may be covalent or ionic in nature. For example, hydrogen is

chemisorbed on nickel. Hydrogen molecules is first adsorbed by van der Waal's forces and then dissociates. The hydrogen atoms are thus chemisorbed on nickel.

2.3.2 Factors affecting Adsorption.

2.3.2.1 Nature of adsorbent

Physical features such as surface area of adsorbent, porosity, particle size, and molecular weight of adsorbent, solubility and ionic radii of species involved all determine the rate of adsorption.

From reaction kinetics theory, the larger the surface area, the higher the reaction rate. This implies that the rate of adsorption will increase when the particle size is small or decreases, this is attributed to the fact that small particle size results in a greater surface area and the more active sites available for adsorption process for a given amount of adsorbent(Gao et al.,2009).

Small particle sizes reduce the inner diffusional and mass transfer limitation to the limitation of the adsorbate inside the adsorbent. Thus equilibrium is easily archived and full adsorption capability is attained. The pore sixe distribution allows for effective migration of contaminants to the point of adsorption.

The solubility of the adsorbate also plays a major role in efficacy of adsorption higher solubility shows a strong solvent interaction. The increase in the interaction in terms of the bond change length increases the hydrophobicity of the molecules hence resulting in a greater adsorption.

2.3.2.3 Contact time or residence time

Interaction between the adsorbate and asorbent, percentage of adsorption is expected to increase until an equilibrium is reached. The time to reach equilibrium depends solely on the adsorbent and adsorbate interaction.

2.3.2.4 Dosage of adsorbent

Dosage influence on removal of metals in water can vary, it is represented in two ways; as the dosage is increased, it also increases the active sites of the adsorbent which significantly increases the adsorption rate, another way however has been proven increase in dosage results in a decrease of the adsorption rate which is as a result of overlapping of active sites which decreases the surface area of adsorbent.

2.3.2.4 pH effect

The pH of a medium is very significant in predicting the efficiency of adsorption. Usually adsorption differs depending on metals that are being adsorbed, some metals are better to adsorb at acidic pH and others at alkaline pH this usually is due to the charge of the ions of the metal being adsorbed.

2.3.2.5 Effect of flow rate

Slower flow rate produces higher empty bed contact time the adsorbate takes longer time to diffuse onto the solid phase of diffusing media. The shape of breakthrough curve of the slower rate curve is more approximate to the ideal break through curve than fast flow curve. The breakthrough curve for fast flow rate deviates from the ideal breakthrough curve and results in larger root mean square error value (Jusoh et al., 2007)

2.3.3 Adsorption isotherm

Adsorption isotherm is a term that is used to describe the relation of equilibrium pressure or concentration of an atom adsorbed with its amount (mass) onto a solid adsorbent at any constant temperature.

It is presented in the form of an equation or graphical curve.

2.3.3.1 Freundlich Adsorption Isotherm

Freundlich proposed an empirical relation in the form of a mathematical equation.

$$\frac{w}{m} = kP^{\frac{1}{n}} \qquad (2.1)$$

This relation is represented in the form of a curve obtained by plotting the mass of the gas adsorbed per unit mass of adsorbent (w/m) against equilibrium pressure (Crittenden, 1998). Freundlich isotherm is not applicable at high pressures**.**

Logarithms on both sides of Freundlich equation (2.2) results;

$$\boldsymbol{log\,\frac{w}{m} = logk + \frac{1}{n} logP} \qquad (2.2)$$

A plot of log (w/m) against log P results in a straight line with slope $1/n$ and intercept log k. However, plots were straight lines at low pressures, while at higher pressure they showed a slight curvature, especially at low temperature. This indicated that Freundlich equation is approximate and does not apply to adsorption of gases by solids at higher pressures (Duong, 1998).

Freundlich Isotherm, using concentration instead of pressure is obeyed by adsorption from solution.

That is,

$$\frac{w}{m} = k \times C_{\frac{1}{n}} \quad (2.21)$$

Taking logs of the above equation (2.21);

$$log\frac{w}{m} = logk + logC \quad (2.22)$$

This implies that a plot of log *w*/*m* vs log *C* must be a straight line.

2.3.3.2 Langmuir Adsorption Isotherm

Langmuir adsorption isotherms determine the maximum capacity of adsorbent. Langmuir's isotherm describing the adsorption of adsorbate (A) onto the surface of the adsorbant (S),

A + S⇆ AS

Where AS represents a solute molecule bound to a surface site on S.

Langmuir isotherm is a model that used intensely at adsorption studies to make comparison between the adsorption capacities of different adsorbents in order to evaluate the efficiency of these adsorbents (CHEM 331L).

Langmuir model is concept of the monomolecular adsorption on homogeneous surfaces. Adsorption has been proved to be a promising technique at waste water treatment. Recently many researchers have proved the capability of agricultural solid wastes as alternative adsorbents instead of commercial activated carbon to remove different classes of pollutants such as dyes, phenols and metals. This review presents the use of agricultural solid wastes as adsorbents to remove different pollutants and the effect of treatment on their efficiency. Adsorbent efficiency related to the physical and chemical properties of adsorbent (CHEM 331L). Langmuir (1916) derived a simple

adsorption isotherm centred on theoretical considerations named after him (Mahmoud, 2012). Langmuir made the following assumptions;

(a) The coat of the adsorbent adsorbed on the solid adsorbent is one-molecule thick.

(b) The adsorbed coat is uniform all over the adsorbent.

(c) There is no contact between the adjacent adsorbed molecules.

Derivation of Langmuir Isotherm

Langmuir considered that the molecules strike a solid surface and are thus adsorbed (Gimbert et al., 2008).

Adsorption from solution generally follows the same principles as laid down for adsorption of gases by solids and is subject to the same factors**.** Thus,

(i) Some adsorbents specifically adsorb certain solutes more effectively than others.

(ii) An increase of temperature decreases the extent of adsorption.

(iii) An increase in surface area increases the extent of adsorption.

(iv) Adsorption of solutes also includes the formation of an equilibrium between the amount adsorbed and the concentration of the solute in solution.

Precise mechanisms of adsorption from solution are not clear. However there is a limit to the adsorption by a given mass of adsorbent and hence possibly adsorption takes place unless a unimolecular layer is formed.

The constants values can be assessed from the intercept and the slope of the linear plot of experimental data of (C_e/Q_e) versus C_e or ($1/Q_e$) versus ($1/ C_e$) or Q_e versus (Q_e / C_e), (Q_e / C_e) versus Q_e, ($1/ Ce$) versus ($1/ Q_e$) (Langmuir, 1918).

The essential feature of the Langmuir isotherm can be expressed by means of R_L, a dimensionless constant referred to as separation factor or equilibrium parameter (Hall et al., 1966). R_L is calculated using following equation (2.3) (Akar et al., 2009).

$$R_L = \frac{1}{1+K_L C_o} \qquad (2.3)$$

The value of separation factor R_L indicates the adsorption process as given:

Unfavourable (R_L >1)

Linear (R_L =1)

Favourable (0< R_L <1)

Irreversible (R_L = 0)

2.4 Adsorbents

Activated carbon is extensively used as an adsorbent, but it is costly and consequently not inexpensive for wastewater treatment (Chandra et al., 2007).Therefore researchers have been interested in investigating the use of various adsorbents that are easily found and can have the same effect as activated charcoal but less expensive and able to remove different types of pollutant.

2.4.1 Limestone

Limestone is a form of sedimentary rock originating in deposits all over the world. It is one of the most worldwide common forms of sedimentary rock, with an estimated 10% of sedimentary rock. It used in an assortment of ways, it consists largely of minerals calcite and aragonite, which are quartz forms of calcium carbonate ($CaCO_3$) .limestone is composed of grains, most grains in limestone are skeletal fragments of marine organisms such as coral or foraminifera. Other carbonate grains containing limestone are ooids, pelois, and intraclast. These organisms secrete shell made of

aragonite or calcite, and leave these shells behind after the organisms die. (E.g. snails, crabs)

Limestone comprises variable amounts of silica in the form of chert (chalcedomy, flint, jasper, etc) or siliceous skeletal fragment (sponge spicules, diatoms, radiolarians) and varying amounts of clay, silt and sand (terrestrial detritus) carried by rivers.

Some limestone types do not consists of grains; and formed completely by the chemical precipitation of calcite or aragonite, i.e. travertine. Secondary calcite may be deposited through super-saturated meteoric waters (ground water that precipitates the material in caves). This produces speleothems, such as stalagmites and stalactites and stalactites. Another form taken by calcite is oolitic limestone, which can be recognized by its granular (oolite) appearance.

Limestone is found to have many of appearances colour and texture (Fig 2.1).

Fig 2.1: An example of a Rock Sample

Limestone is made up of the mineral calcium carbonate, although it is frequently mixed with other minerals. Impurities usually alter the texture and nature of the limestone with its colour varying according to the rock. Limestone, can be both chalk and marble, with very different feel and physical outlook.

Nearly all limestone are collectively made-up of minute particles of material compressed together, some are known to have crystalline arrangements when magnified. The differences that come with the structures are normally attributed to the way the rock was formed, this also attributes to the color. Limestone is known to have various colours these include the most common ones around which are; yellow, white, brown and black impurities also play a vital role in the colour of the rock. Color variations over the years is known to occur due to the seepage of many solutions through the limestone bedrock (Fookes, 1988).

Several variations of limestone consist of marble, dolomite, and oolite. Manufacturing of many products such animal feed and cement, construction and the preparation of printing plates and other industrial processes are the many uses of limestone.

2.5 UV Spectrometry.

In analytical chemistry, UV spectroscopy is very vital. It comprises the promotion of the electrons from the ground state to the higher energy or excited state. Absorption spectroscopy in which light of ultra-violet region (200-400 nm.) is absorbed by the molecule is the principle behind it. The Ultraviolet radiations are adsorbed and result in the excitation of electrons to a higher state from the ground state. As a result the absorbed energy is the same as the energy difference between the ground state and higher energy states (Aman Thakur, 2011).

2.5.1 UV spectroscopy Principle

UV spectroscopy follows the Beer-Lambert law, which states that: when a beam of monochromatic light is passed through a solution of an absorbing substance, the rate of decrease of intensity of radiation with thickness of the absorbing solution is

proportional to the incident radiation as well as the concentration of the solution (Aman Thakur, 2011). The expression of Beer-Lambert Law is:

$$A = log\left({}^{I_o}/_{I}\right) = ECL$$

Beer-Lambert law is clear that the larger the number of molecules capable of absorbing light of a given wavelength, the larger the extent of light absorption. This is the basic principle of UV spectroscopy (Aman Thakur, 2011).

2.5.2 Instrumentation and working of UV spectroscopy

I. **Light Source-** Tungsten filament lamps and Hydrogen-Deuterium lamps are most widely used and suitable light source as they cover the whole UV region. Tungsten filament lamps are rich in red radiations; more specifically they emit the radiations of 375 nm, while the intensity of Hydrogen-Deuterium lamp17s falls below 375 nm (Aman Thakur, 2011).

II. **Monochromator**- Monochromators generally composed of prisms and slits. The most of the spectrophotometers are double beam spectrophotometers. The radiation emitted from the primary source is dispersed with the help of rotating prisms. The various wavelengths of the light source which are separated by the prism are then selected by the slits such the rotation of the prism results in a series of continuously increasing wavelength to pass through the slits for recording purpose. The beam selected by the slit is monochromatic and further divided into two beams with the help of another prism (Aman Thakur, 2011).

III. **Sample and reference cells**- One of the two divided beams is passed through the sample solution and second beam is passé through the reference solution.

Both sample and reference solution are contained in the cells. These cells are made of either silica or quartz. Glass can't be used for the cells as it also absorbs light in the UV region (Aman Thakur, 2011).

IV. **Detector-** Generally two photocells serve the purpose of detector in UV spectroscopy. One of the photocell receives the beam from sample cell and second detector receives the beam from the reference. The intensity of the radiation from the reference cell is stronger than the beam of sample cell. This results in the generation of pulsating or alternating currents in the photocells (Aman Thakur, 2011).

V. **Amplifier-** The alternating current generated in the photocells is transferred to the amplifier. The amplifier is coupled to a small servometer. Generally current generated in the photocells is of very low intensity, the main purpose of amplifier is to amplify the signals many times so we can get clear and recordable signals (Aman Thakur, 2011).

VI. **Recording devices**- Most of the time amplifier is coupled to a pen recorder which is connected to the computer. Computer stores all the data generated and produces the spectrum of the desired compound (Aman Thakur, 2011).

2.5.3 UV spectroscopy applications

(a) Detection of functional groups- UV spectroscopy is used to detect the presence or absence of chromophore in the compound. This is technique is not useful for the detection of chromophore in complex compounds (Aman Thakur, 2011). Functional groups can be detected by the observing of bands being present, if these band are present it indicates a particular group is present and the opposite id the same if it is not present. Spectrum readings of compound which are

transparent above 200 nm indicate the absence of ,conjugation, carbonyl groups, benzene, aromatic compounds bromine and iodine atoms

(b) UV Spectroscopy is used in the detection of the type of conjugation that is present in compounds. With the increase in double bonds the absorption shifts towards the longer wavelength. If the double bond is increased by 8 in the polyenes then that polyene appears visible to the human eye as the absorption come in the visible region.

(c) Identification of an unknown compound- An unknown compound can be identified with the help of UV spectroscopy. The spectrum of unknown compound is compared with the spectrum of a reference compound and if both the spectrums coincide then it confirms the identification of the unknown substance.

(d) Determination of configurations of geometrical isomers- It is observed that cis-alkenes absorb at different wavelength than the trans-alkenes. The two isomers can be distinguished with each other when one of the isomers has non-coplanar structure due to steric hindrances. The cis-isomer suffers distortion and absorbs at lower wavelength as compared to transformer.

(e) Determination of the purity of a substance- Purity of a substance can also be determined with the help of UV spectroscopy. The absorption of the sample solution is compared with the absorption of the reference solution. The intensity of the absorption can be used for the relative calculation of the purity of the sample substance (Aman Thakur, 2011).

2.6 Batch Systems

Contact adsorption systems have long been used to remove pollutants from wastewater (McKay, 1996). Such systems consist of a batch reactor in which the effluent (e.g.

wastewater) and the adsorbent are intimately mixed for a certain time to enable the system to approach equilibrium. The time required for the adsorbent and liquid to come to substantial equilibrium depends primarily on the concentration and particle size of the solid, the viscosity of the liquid, solute concentration and the extent of agitation (McKay, 1981). For a single-stage adsorption system, the mass balance at Equilibrium is:

$$V \times (C_o - C_1) = M \times S \qquad (2.4)$$

Where V (L) is the volume of solvent having a solute concentration of C (g L^{-1}) and M (kg) is the amount of adsorbent. The solute concentration in solution is reduced from C_o to C_1 (g L^{-1}) and becomes adsorbed to the solid at a concentration S (g kg^{-1}). Similar batch adsorption systems have been used at laboratory scale to assess the ability of CCBM (Calcium carbonate based materials) to attract iron (Wang Yu, 2013).

Batch experiments (Fig. 2.2) carried out to determine the adsorption isotherms of metal ions onto the adsorbents in glass flasks. The flasks are shaken at a constant rate, allowing sufficient time for adsorption equilibrium. It was assumed that the applied shaking speed allows all the surface area to come in contact with heavy metal ions over the course of the experiments. The study is performed at room temperature to be representative of environmentally relevant condition. All experiments were carried out in duplicate and the average value was used for further calculation. The pH of the solution is measured with a pH meter and the flasks were plugged and kept closed to avoid the fluctuation of pH due to the exchange of gases during the experiment. The effects of various parameters on the rate of adsorption process are observed by varying contact time, adsorbent concentration, temperature, and pH of the solution. The solution volume is usually kept constant unless it is a parameter being measured (Gupta, 1998)

The amount of metal adsorbed per unit mass is calculated so are the initial and equilibrium concentration (mg/L), the mass of the adsorbent (g) and the volume of the solution (mL). Percent metal ion removal (%) is calculated using the equation.

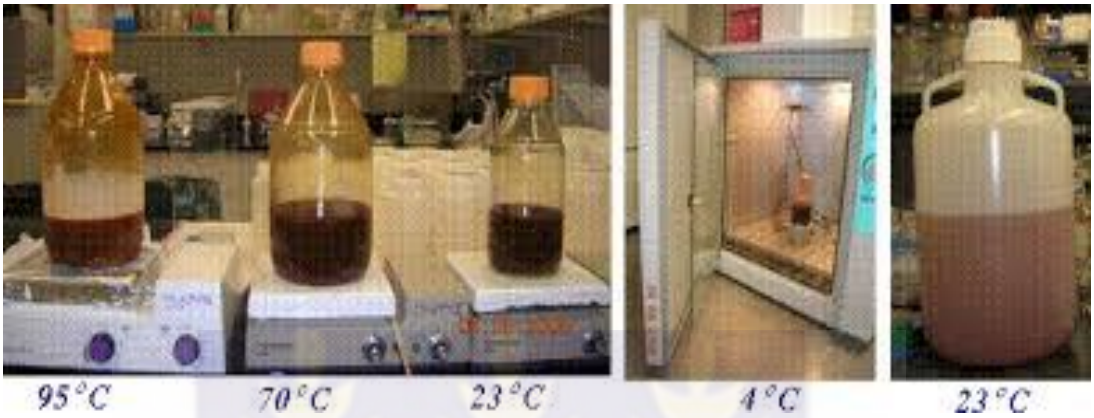

Fig 2.2: Batch experiments being conducted on orbital shakers

Column Test

The adsorption experiments are carried out in columns that were equipped with a stopper for controlling the column flow rate. This experiment is useful in understanding and predicting the behaviour of the process. The sample solution is passed through the adsorption column with a known absorption usually at a flow rate of 6 mL/min by gravity. The flow rate is kept constant by controlling the stopper valve.

2.7 Natural Background Radioactivity

Natural radioactivity originates from the earth's crust and outer space (terrestrial and cosmogenic). These sources are from the Uranium series (U-238), Thorium series (Th-232) and Potassium (K-40). In addition to the Naturally Occurring Radioactive Material (NORMS). Anthropogenic activities introduce man made radioactive radionuclides into the environment due to proliferation of different nuclear applications.

Natural background radiation levels differ from place to place and are a function of properties of the underlying rocks and of the soil in the location, such as distribution of

uranium and radium porosity, permeability, moisture content as well as meterological and seasonal variation (Merdanoglu and Altinspy, 2006; Chowdhury et al., 2004).

2.8 Gamma spectrometry

Gamma ray spectrometry is an analytical method that allows the identification and quantification of gamma emitting isotopes in a variety of samples. A typical analog HPGe detector-based gamma spectroscopy system (Fig. 2.3) consists of a HPGe detector, high voltage power supply, preamplifier (which is usually sold as part of the detector), amplifier, Analogue to Digital Coverter (ADC), and Multi-Channel Analyzer (MCA) [Fig. 2.4] (Faanu et al., 2013).

The electronic system collects the electrons produced from the signal pulses, processes the pulses and sorts them by height or energy. This process can be described by the following steps

- Photon interacts with the detector crystal, produces burst of electrons
- Applied bias voltage sweeps electrons from crystal
- Current produced by electrons forms signal pulse
- Pulse size is increased with a preamplifier
- Pulse is further intensified and shaped with amplifier
- Pulse intensity is converted into numerical value using ADC
- Numerical values are sent

In a single measurement and with minimum sample preparation, gamma ray spectrometry enables the detection of several gamma emitting radio nuclei in given samples (Faanu et al., 2013). The measurement gives a spectrum of lines, the amplitude of which is proportional to the activity of the radionuclide and its position on the

horizontal axis gives an idea on its energy. It is a widely used analysis method for quantifying nuclide specific radioactivity in samples (Anspaugh, 1976).

This method makes use of emitted gamma radiation, by a sample, which is produced during the decay of radionuclides. Gamma spectrometry provides no information on potential radioactive contaminants that emit only beta- or alpha radiation and whose presence cannot be inferred from short-lived gamma emitting daughter radionuclides, such as ^{90}Sr.

Fig 2.3: Examples of γ-ray detectors

Sample sizes required are usually in the range of grams to several kilograms. It is evident, that the smaller the sample size the larger the increase of the measuring time for getting the same analysis accuracy.

Fig 2.4: Typical example of a gamma spectrometer setup

Sample size analysis for gamma is in general larger than that required for gross alpha/beta analysis; hence sub-sampling errors will be smaller and results are more representative of in-situ conditions. Activities of common man-made radionuclides, such as ^{137}Cs and ^{60}Co, and of natural series decay chains (headed by ^{235}U, ^{238}U and ^{232}Th) can be measured or inferred. In the case of samples contaminated with natural series, e.g., phosphate ores, zirconium, etc. The measurements decay chains are to be measured in equilibrium (United Nations Scientific Committee on the Effects of Atomic Radiation, 2000)

However, not all radionuclides will be detected using gamma spectrometry. For example, radionuclides emitting very low gamma fluxes and/or pure alpha- and/or beta radiation. The technique is not used in isolation unless the radionuclide fingerprint of the contaminated site is well understood and there is confidence that total levels of radioactive contamination can be derived from the gamma spectrometry data (Fig. 2.5).

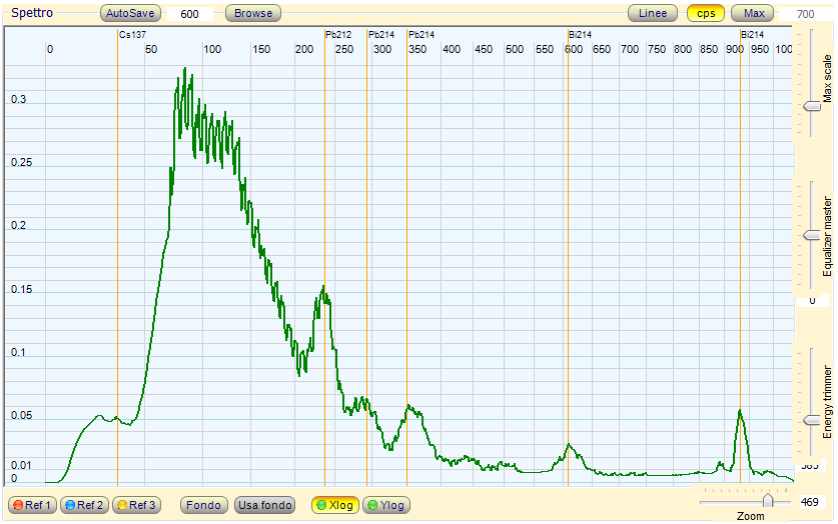

Fig 2.5: Typical example of a spectrum of gamma spectroscopy

For liquids, gamma spectrometry is used to provide detailed analysis of contaminated samples. This is as a result of gross alpha/beta analysis of waters provides accurate and precise measurement of detection limits below activity levels that are of radiological concern (Velzen.2004).

The detection limits of gamma spectrometry typically exceed those of the gross/alpha/beta technique.

Gamma spectrometers are screened against background radiation to improve the minimum detectable activity of measurements [Velzen.2004]. (The level of radon daughters inside a shield can be reduced further by allowing the liquid nitrogen Dewar which is used to cool high resolution gamma spectrometers to vent into the shield, thereby purging room air and replacing it with clean gas.)

2.9 Accelerator

A particle accelerator is a machine that accelerates elementary particles, such as electrons or protons, to very high energies. On a basic level, particle accelerators produce beams of charged particles that can be used for a variety of research purposes. There are two basic types of particle accelerators: linear accelerators and circular

accelerators. Linear accelerators propel particles along a linear, or straight, beam line. Circular accelerators propel particles around a circular track. Linear accelerators are used for fixed-target experiments, whereas circular accelerators can be used for both colliding beam and fixed target experiments (Dobbs, 2011).

Its essential principle is some form of loaded waveguide, in which an oscillating field of high amplitude can be set up, which can be analysed into traveling waves, one of which travels with the velocity of the particle to be accelerated. Particles in the correct phase can then remain always in the phase of the traveling wave corresponding to acceleration, and can pick up energy continually, just as if they were in a constant field. If the properties of the field are arranged to vary, as the particle goes along the tube, so as to keep step with the acceleration of the particle, energies of any amount can in principle be acquired.

2.9.1 How a particle accelerator works

Particle accelerators use electric fields to speed up and increase the energy of a beam of particles, which are steered and focused by magnetic fields. The particle source provides the particles, such as protons or electrons that are to be accelerated. The beam of particles travels inside a vacuum in the metal beam pipe. The vacuum is crucial to maintaining an air and dust free environment for the beam of particles to travel unobstructed (Fig. 2.6). Electromagnets steer and focus the beam of particles while it travels through the vacuum tube. Electric fields spaced around the accelerator switch from positive to negative at a given frequency, creating radio waves that accelerate particles in bunches. Particles can be directed at a fixed target, such as a thin piece of metal foil, or two beams of particles can be collided. Particle detectors record and reveal the particles and radiation that are produced by the collision between a beam of particles and the target (Das, 2003).

2.9.1.1 Element composition

- At the accelerator, the samples are bombarded with high energy photons resulting in;
    i. atoms extracted from a sample are ionized,
    ii. accelerated to high energies,
    iii. separated according to their momentum, charge and energy
    iv. Then individually counted.

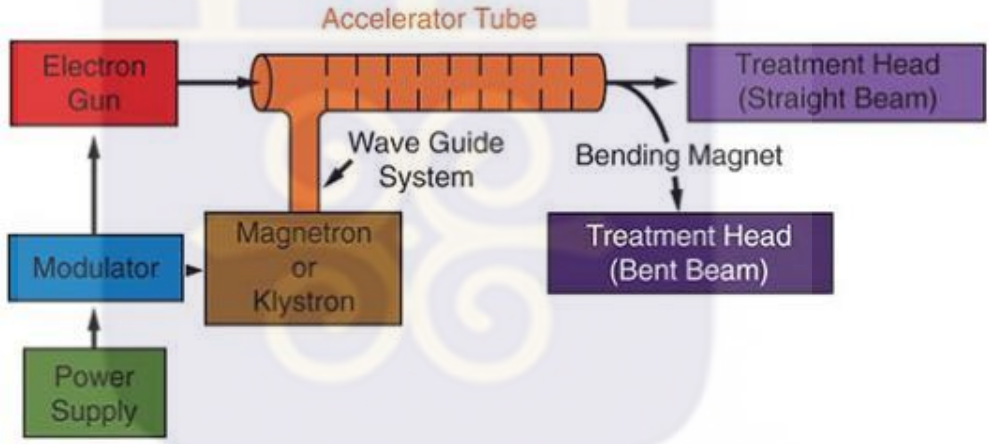

Fig 2.6: Block diagram of a typical accelerator setup

Standard samples are used to calibrate the instruments and compare the obtained results, the final percentages are calculated as weight percentage of each element or compound to the sample weight.

CHAPTER THREE

METHODOLOGY

This chapter describes the laboratory experiments conducted towards achieving the purposes of the study.

3.1 Limestone Collection Site

3.1.1 Geographical location of Yilo Krobo-Otekpolu

Oterkpolu, (0^o 05' W; 6^o 15' N), is a farming community and one of the twenty-two (22) communities located in the Yilo Krobo Municipality (between latitude 6000'N and 0030'N; and longitude 0030'E - 1000'W). Oterkpolu is about 1.5 km off the Koforidua-Asesewa main road. Out of the estimated 87,847 population of the Yilo Krobo Municipality, the population of Oterkpolu constitutes about 1.7% (1500 people) [Ghana Statistical Service, GSS, 2010]. The Municipality covers an estimated area of 1201 sq km and is predominantly rural (more than 67% of its population live in rural communities). The major economic activities in the Municipality are Agriculture, Trading and Small Scale Industrial activities (like Beads Making) [Yilo Krobo Municipal Profile, 2006]

With Somanya as the administrative capital of the Yilo Krobo Municipality, the municipality shares boundaries with New Juabeng and East Akim Municipalities to the west, Lower and Upper Manya Krobo to the north and east respectively, Akuapem North and Dangme West municipalities to the south.(GSS,2010).

The municipality is about 80% mountainous with the Akuapem Range stretching from the southwest to northeast with numerous valleys across the municipality. The Togo series (including quartzites, phyllites, sandstones, phyllonites and sandy-shades) forms

the rocks of the range peaking at an average height of between 300-500 meters above sea level.(Mofa,2015)

3.1.2 The Oterkpolu Limestone Deposit

The limestone deposit is located about 6.5 km east of Oterkpolu Township about 25 km from Koforidua, the Eastern regional capital (Fig. 3.1). The limestone occurs within the arenaceous rocks of the Lower Voltaian range. The limestone is overlain by brown sandstone containing small iron-rich concretions which are weathered out to give a characteristic pitted surface with a purplish coloured transition zone at the base of the limestone. The rocks dip eastward into the hillside with local variation occurrences due to folding. Investigations by the Ghana Geological Survey have estimated the limestone reserve at Oterkpolu to be over 3.7 million tonnes.

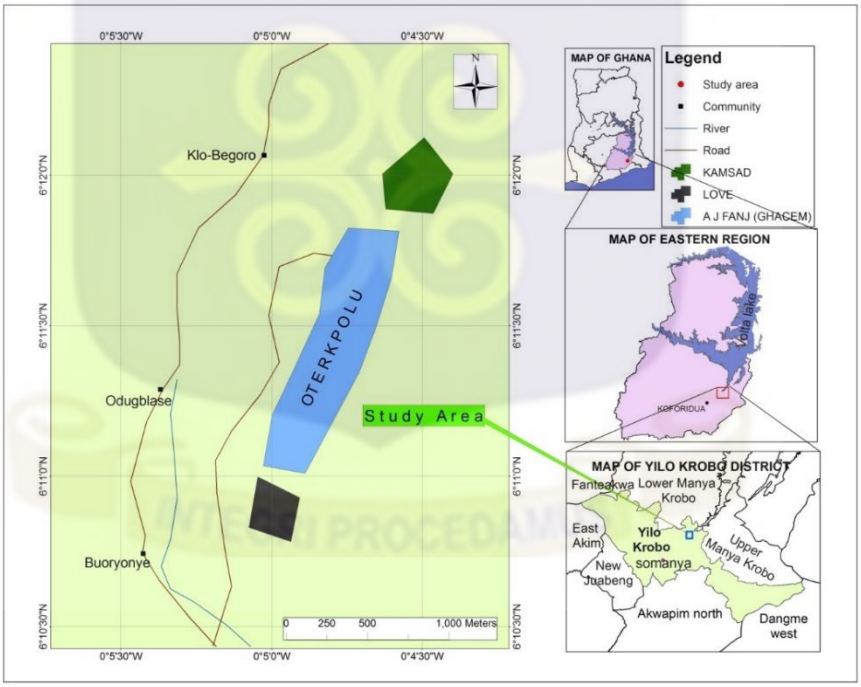

Fig 3.1: Map of limestone deposit site

3.1.3 Collection of Limestone

A quarry rotary air drill was used to find the hanging wall and the foot wall of the deposit between core holes. Limestone samples were taken at intervals this was

necessary to locate the quality a shovel was used to put the limestone in polythene bags. Each limestone sample was labelled first then bagged in a polythene rubber and then in sacks to prevent weathering. The limestone samples are then transported to the laboratories of Ghana Atomic Energy Commission in Kwabenya, Accra.

3.2 Preparation of Limestone Samples

3.2.1 Crushing of rock samples

Rock samples were taken to the meterogical department were they were crushed and grind into 3 different sizes 500-1000, 1000-2000, 2000-6300 µm, this was done using a Stone crushing motor to increase the surface area of the limestone which was to be used in the experiment.

3.2.2 Sample Composition of Limestone

High quality of limestone with high calcium (Ca) is required for excellent adsorption; accordingly, assessment of the elemental composition of the limestone was undertaken. The rock samples were therefore, taken to the Department of Earth Science, University of Ghana, Main Legon campus, Accra. At the laboratory, an Abrasive Saw was used to cut the rocks into 1 cm by 0.03 cm length by breath. This was done so as to make the samples thin enough for the composition to be easily determined while using the Ion beam accelerator (recommended sample size for sample holders)

- Two specific limestone samples were selected to be analysed EKLRO2 (Grey in colour) and EKLD01 (Reddish in colour). These samples were then taken to the laboratories of the Ghana Atomic Energy Commission in Kwabenya, Accra, and were tested for composition both compound analysis and elemental analysis were done Silicon (Si), Potassium (K), Calcium (Ca), Iron (Fe), Manganese (Mn), Zinc (Zn) and Sulphur (S) were tested with much emphasis on the iron

and calcium content available in the samples. At the Accelerator Centre, the samples are bombarded with high energy photons resulting in;

i. atoms extracted from a sample are ionized,

ii. accelerated to high energies,

iii. separated according to their momentum, charge and energy

iv. individually counted.

Standard samples are used to calibrate the instruments and compare the results, the final percentages are calculated as weight percentage of each element or compound to the sample weight.

3.3 Radiological Safety of the Limestone Deposits

3.3.1 Instrumentation

Fig 3.2: Sealed (radon impermeable tapes) Marinelli beakers containing the samples

3.3.2 Sampling and Sample Preparation of Limestone for Gamma Spectrometric Analysis

In the laboratory, samples were homogenised and transferred into 0.5 L Marinelli beakers (Fig. 3.2). These beakers were completely sealed using radon impermeable tapes and stored for three (3) weeks, for the short-lived daughters to reach equilibrium with their long-lived parent radionuclides 238U and 232Th (ASTM, 1983; 1986). Sealed sample in the Marinelli beaker weighed and placed on the HPGe γ-ray semi-conductor detector for measurement of NORMs. Measurement time was 36000 Seconds. Experimental set-up presented in Fig 3.3.

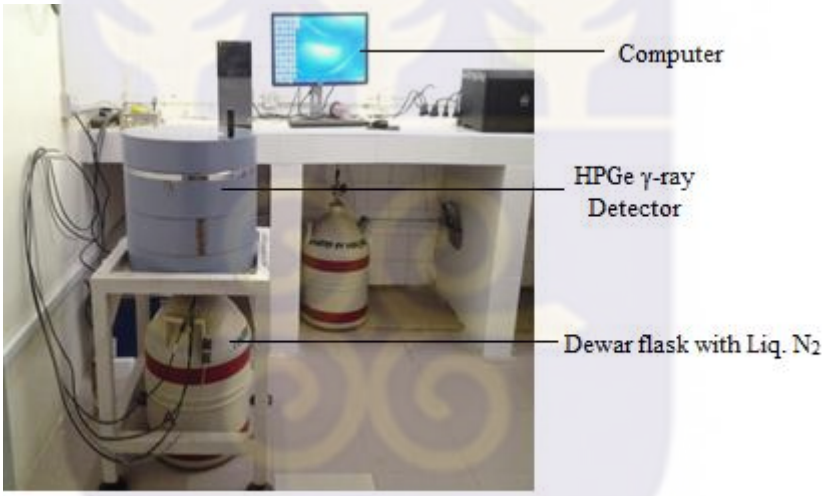

Fig 3.3: HPGe Gamma Spectrometer

3.3.3 Instrumentation and calibration

Straight gamma spectrometry non-destructive examination was used for the measurement of gamma rays for the limestone samples using a High Purity Germanium detector (HPGE). The gamma spectrometry system was made up of HPGE detector attached to a computer based multi-channel analyser (MCA). The comparative efficiency of the detector was 40 % with energy resolution of 2.0 keV at gamma ray

energy of 1332 keV of 60Co. The identification of each radionuclides was done using their characteristic gamma-ray energies and the quantitative analysis of radionuclides was done using the Genie 2000 gamma acquisition and analysis software. The detector was housed in a 100 mm passive shielding of lead lined with copper, cadmium and 3mm Plexiglas to lessen the background radiation. The detector was cooled in liquid nitrogen at a temperature of -196 0C (77 k). To determine the background distribution around the detector (quality control), ten (10) empty Marinelli beakers were carefully prepared using nitric acid and counted for 36000 s as the samples. The background spectra were used to correct the net peak area of gamma rays of calculated isotopes. The background spectra were also used to define the minimum detectable activities of radionuclides at each photo peak for the detector.

Energy calibration (Fig. 3.4) was done by counting standard radionuclides of known activities with defined energies in the energy range of 60 keV to ~2000 keV using standard radionuclides uniformly dispersed in solid water with volume and density of 1000 cm^3 and 0.98 g cm^{-3} respectively (Source number: 9031-OL-146/14 and manufactured by Czech Metrology Institute).

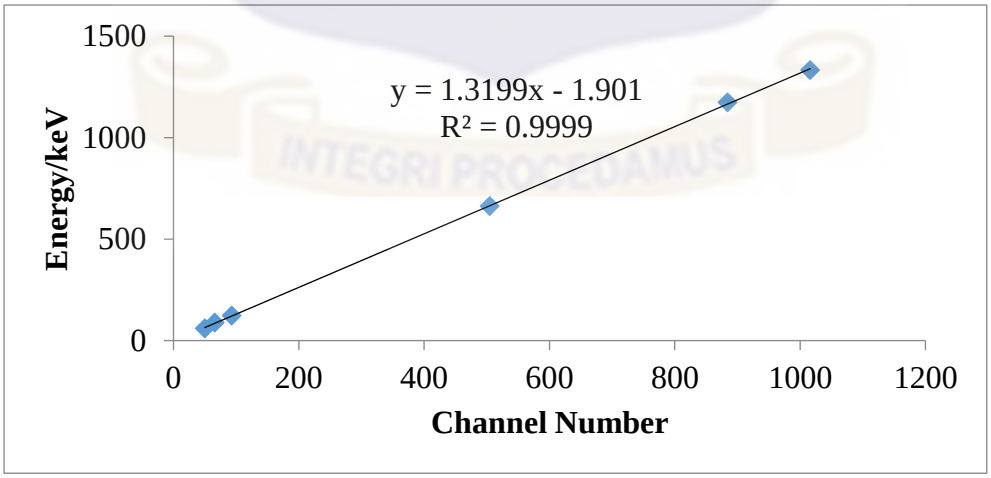

Fig 3.4: Energy calibration line

$$E = A_0 + A_1 \cdot CN \quad (3.1)$$

From equation *(3.1)* E is the energy (keV), CN is the channel number for each radionuclide, and A_0 and A_1 are calibration constants.

The IAEA reference materials IAEA-RGU-1(U-ore), IAEA-RGTh-1 (Th-ore) and IAEA-RGK-1 (K-ore) with densities (1.33 ± 0.03) similar to the samples to be measured were prepared into same cylindrical containers as that of samples for the efficiency calibration of the gamma system.

Efficiency calibration

The efficiency calibration was executed by obtaining a spectrum of the standard until the count rate of total absorption could be calculated with a statistical uncertainly of <1% at a confidence level of 95%.

The net count rate was determined at the photo peaks for all the energies to be used for the determination of the efficiency of the calibration standard at the measurement time. The efficiency at each energy was plotted as a function of the peak energy and extrapolated to determine the efficiencies at other peak energies for the measurement geometry used. The efficiency was related to the count rate in addition to the activity of the standard by the relation from Gilmore (equation 3.2):

$$\eta = \frac{N}{P_\gamma \times T_c \times A} \quad (3.2)$$

Where η is the efficiency of the detector, N is the total count under a photo peak $P\gamma$ is the gamma ray emission probability for the energy, in a peak range, A is the activity of the calibration standard for each radionuclide in Bq at measurement time while T_c being counting time.

$$(E) = a_0 + a_1 lnE_1 + a_2 lnE_2 \quad (3.3)$$

Equation (3.3) is the relation of efficiency to the energy expression;

Where a_0, a_1 and a_2 are calibration constants. The efficiency calibration curve is shown in Fig. 3.5.

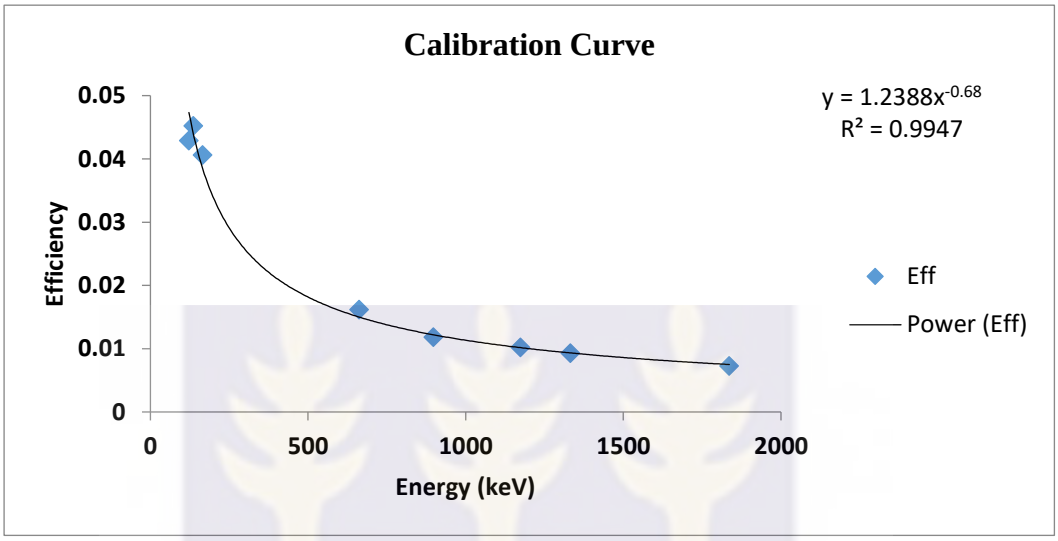

Fig 3.5: Efficiency calibration curve

From the calibration curve, the expression using a first order polynomial (equation 3.4):

$$\ln\eta = 1.239 - 0.995\ln E\gamma \qquad (3.4)$$

For E_γ > 100 keV

Calculation of Activity Concentration and Estimation of doses

"The activity concentrations of ^{226}Ra were determined using the γ-ray emissions and the respective γ-yield of ^{214}Pb at 351.9 keV (35.8%) and ^{214}Bi at 609.3 keV (44.8%). The ^{228}Ra activity concentrations were determined through the gamma emissions of ^{228}Ac at 911 keV (26.6%), and the ^{228}Th activity concentrations were determined through the gamma emissions of ^{212}Pb at 238.6 keV (43.3%) and ^{208}Tl at 583 keV (30.1%) and 2614.7 keV (35.3%) taking into consideration a branching ratio of 33.7% from ^{212}Bi towards ^{208}Tl. The ^{40}K activity concentration was determined directly from

its emission line at 1460.8 keV (10.7%) while the ^{137}Cs and ^{210}Pb activity concentrations were determined directly from the gamma emission lines at 661.67 keV (85.1%) and 46.5 keV (4.3%) respectively. Finally, the ^{238}U activity concentrations were determined through the gamma-ray emission of its daughter ^{234}Th (4.8%). All the energies and intensities of the different radiations mentioned were taken from a well-known library" (Fig. 3.6).

The analytical expression used in the calculation of the activity concentrations in Bqkg-1 for The analytical expression used in the calculation of the activity concentrations in Bqkg^{-1} for sludge and oil based mud and in BqL^{-1} for waste water samples as shown in equation (3.5).

$$A_{sp} = \frac{N_D}{p.T_c.\eta(E).M} \qquad (3.5)$$

where; N_D is the net counts of the radionuclide in the samples, p is the gamma ray emission probability (gamma ray yield), T_c is the sample counting time, $\eta(E)$ is the absolute counting efficiency of the detector system, M is the mass of the sample (kg) or volume (L)

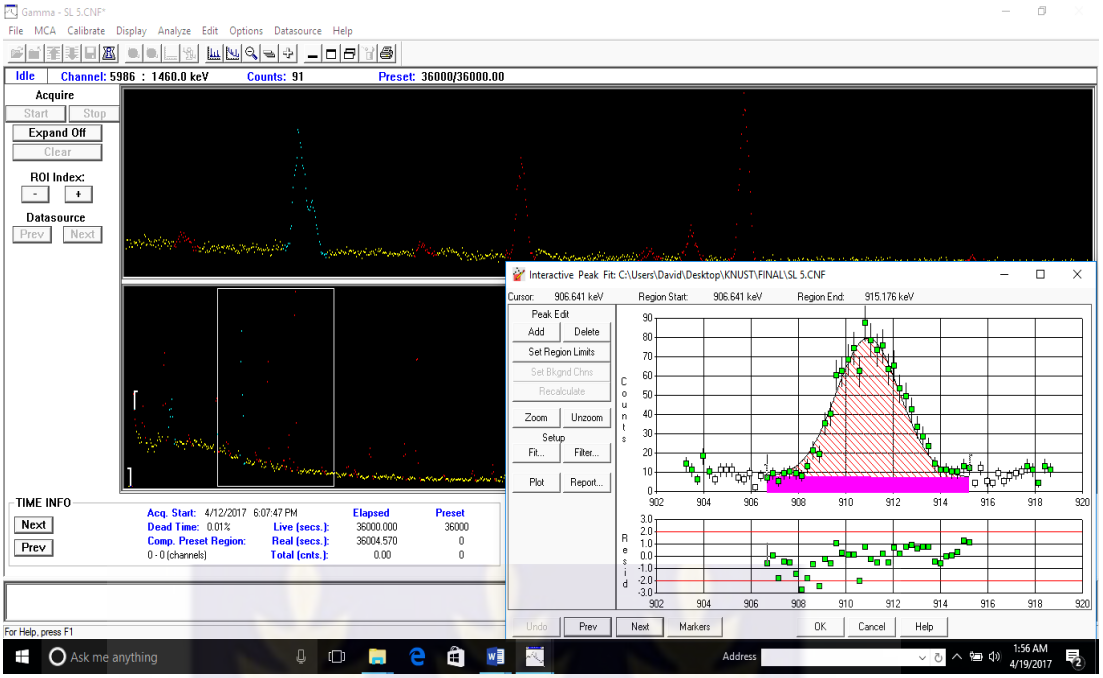

Fig 3.6: Genie 2000 gamma acquisition and analysis software interface

Calculation of Absorbed Dose Rate (ADR)

From the mean specific concentrations of U-238, Th-232 and K-40, the dose rate will be determined using the relation (equation 3.6) from Beck et al., 1992;

$$\boldsymbol{ARD = 0.417C_U + 0.462C_{Th} + 0.604C_K} \qquad (3.6)$$

Where $\boldsymbol{C_U}$, $\boldsymbol{C_{Th}}$ *and* $\boldsymbol{C_K}$ are the specific concentrations of U-238, Th-232 and K-40 in Bq/kg

3.3.2.5 *Calculation of Annual Effective Dose (AED)*

The annual effective dose due to the absorbed dose rate was calculated using the relation (equation 3.7);

$$\boldsymbol{AED = ARD \cdot \frac{8760hr}{yr} \cdot 0.2 \cdot 0.\frac{7Sv}{Gy} \cdot 10^{-6}} \qquad (3.7)$$

Where the outdoor occupancy is 0.2 as suggested by UNSCEAR, 2000 and 0.7 Sv/Gy being the dose conversion factor.

3.4 Batch Adsorption Experiment

3.4.1 Apparatus/Materials

Measuring cylinder (50 and 100 mL), Orbital shaker, Magnetic stirrer (Eisco EI 0112M, India), Beakers, Sampling bottles, 1 mL Syringe (Ningbo Clan Medical Instruments Co, Ltd, India), PTFE Syringe Filter-0.45 µm (Filter-Lab, UK), Volumetric flask (1000 and 100 cm^3), Mettler AB204-S analytical balance (Mettler Toledo).

3.4.1.1 Standards

An Iron Stock solution (1000 mg/L) [Fizmerk, India] was prepared by diluting 25 mL of 1000 mg/L standard Iron solution in a 250 mL volumetric flask with distilled water and adding to the mark. A Working standard of concentration 10 mg/L was prepared by appropriate dilution of the stock.

Using the dilution method formula [equation (3.8)];

$$\boldsymbol{M_1V_1 = M_2V_2} \qquad (3.8)$$

Where $\boldsymbol{M_1}$ and $\boldsymbol{M_2}$ are masses in (mg); $\boldsymbol{V_1}$ and $\boldsymbol{V_2}$ are volumes in (L)

3.4.1.2 Reagents

10 mg/L working solution was preferred because the standard solution would have a distinct observation of the change after being subjected to the technique.

3.4.2 Experimental Procedure

The concentrations of the prepared solutions (stock and dilute) were ascertained using a Jenway 6305 UV spectrometer. This was to make sure the dilutions and calculations were accurate.

3.4.2.1 Sample Size Analysis

50 grams aliquot of the raw crushed limestone of different grain sizes (500-1000 µm, 1000-2000 µm and 2000-6350 µm) were each weighed with Mettler AB204-S analytical balance as shown in Fig 3.7

Fig 3.7: Weighing of limestone sample using a Mettler AB204-S analytical balance

Into a 250 mL beakers and were each mixed with 200 mL of standard solution. The pH of each beaker was measured and each mixture was magnetically agitated for 60 minutes with an Eisco EI 0112 M Magnetic Stirrer at 350 rpm and settling time 20 minutes. 10 mL of the mixture was taken and the residual iron concentration determined

using a Jenway 6305 UV spectrometer. A blank was prepared by mixing 50 g limestone with 200 mL of distilled water and agitating it magnetically as well.

Table 3.1: Data for various parameters kept constant while the sample size is varied.

Parameter	**Beaker**			**Blank**
	1	2	3	
Mass of Limestone (g)	50	50	50	50
pH (of water)	6.48	7.31	7.38	7.06
Concentration of iron (mg/L)	10	10	10	10
Size of limestone (µm)	2000-6350	1000-2000	500-1000	500-1000
Time shaken (min)	60	60	60	60
Volume of water (mL)	200	200	200	200

The removal of iron efficiency of the limestone sample was determined by measuring the initial and residual iron concentrations in the various aliquots taken and calculated as follows;

$$\textbf{\% Adsorption} = \frac{C_o - C_t}{C_o} \times \mathbf{100} \qquad (3.9)$$

$$\textbf{Adsorption Capacity} = \frac{C_o - C_t}{M} \times \mathbf{V} \qquad (3.10)$$

Where; C_o = initial iron concentration (mg/L)

C_t = residual iron concentration (mg/L)

M = mass of adsorbent used (mg)

V = volume of fluoride solution used in Batch experiment (L)

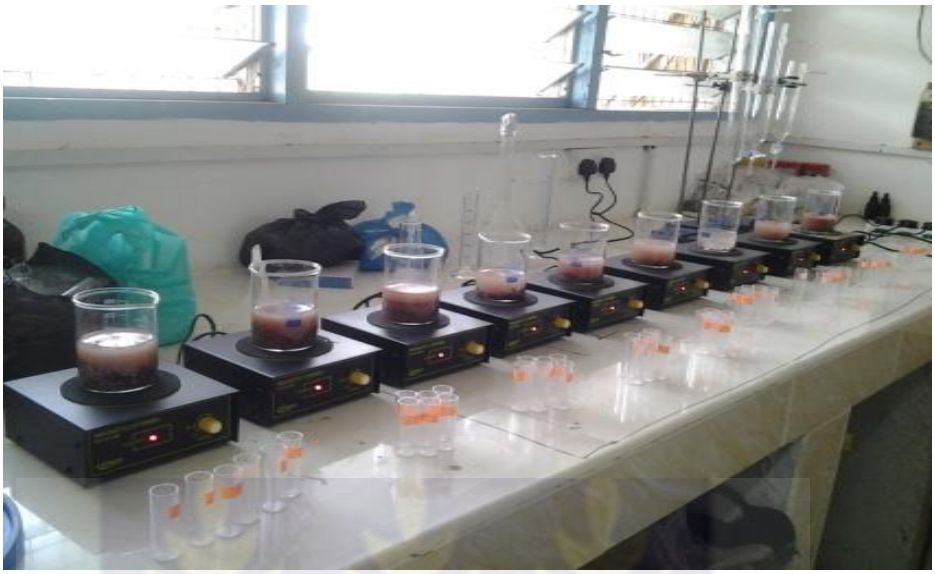

Fig 3.8: Batch setup showing mixtures agitated by magnetic stirrer on orbital shakers

3.4.2.2 Effect of Varied Dosage

To determine the effect of varied dosage batch adsorption experiments were conducted these ranged from 20 to 100 g mass of limestone in 200 mL of standard solution just as it was done for sample size analysis every parameter was kept constant except the dosage (Table 3.1).

In this experiment, various dosage were put into a 250 mL beaker and shaken using orbital shaker with a magnetic stirrer in the beakers (shak ing speed = 350 rpm, contact time = 60 minutes and settling time 20 minutes) [Fig 3.8]. After 20 minutes of settling time, 10mL of samples were drawn from supernatant for Iron analysis using a Jenway 6305 UV spectrometer.

3.4.2.3 Effect of Varied Time

The experiment was conducted by shaking 50 g limestone sample in 200 mL of standard solution in each 250 mL beaker. The aim of this experiment is to determine the optimum contact time required for maximum removal of Fe. The effect of various contact times (60, 90, 120 minutes) was studied. The beakers were agitated at 350 rpm. After shaking process, the samples were allowed to settle for 20 minutes; 10 mL of sample were drawn and thus were analysed using Jenway 6305 UV spectrometer.

3.4.2.4 Effect of Varied pH

The experiment was conducted by shaking 50 g limestone sample in 200 mL of standard in each 250 mL beaker. Different pH was set for each beaker pH 3, 5, 8, 9, 12 were used in the experiment the pH was reduced by adding acid HCl and increased by adding a base NaOH.

The purpose of the experiment was to determine the influence of pH on the removal of iron from drinking water.

A UV spectrometer was used in the determination of the iron concentration

- The samples were run in triplicates to obtain consistent results.

3.5 Derivation of Calibration Curve for Jenway 6305

Five aliquot concentrations were prepared from an Iron standard after which FerroVer Iron reagent powder pillow was added to each solution for an orange colour development. The orange colour developed indicates the presence of iron and the intensity of the colour increases due to the concentration of the iron in the solution increasing. The respective absorbances of these solutions were calculated at a wavelength 510 nm from the UV-Visible spectrophotometer to generate the calibration

curve (Fig. 3.9) from which the subsequent sample analysis was subjected to extrapolate their respective concentrations (Table 3.2).

NOTE: The water used in the preparation of the various aliquot concentrations of the Iron standard was firstly measured at 510 nm from the UV-Visible Spectrometer (blank) and its absorbance was subtracted from the absorbance of each aliquot concentration of the Iron standard to afford the corrected absorbance of each concentration.

Table 3.2: Data for absorbance of different iron standards

Iron standards (mg/L)	Absorbance (A) Iron standards	Absorbance (B) Blank	Corrected Absorbance (A-B)
0.2	0.0041	0.0013	0.0028
0.4	0.005	0.0013	0.0037
0.6	0.0073	0.0013	0.006
0.8	0.0096	0.0013	0.0083
1	0.0129	0.0013	0.0116

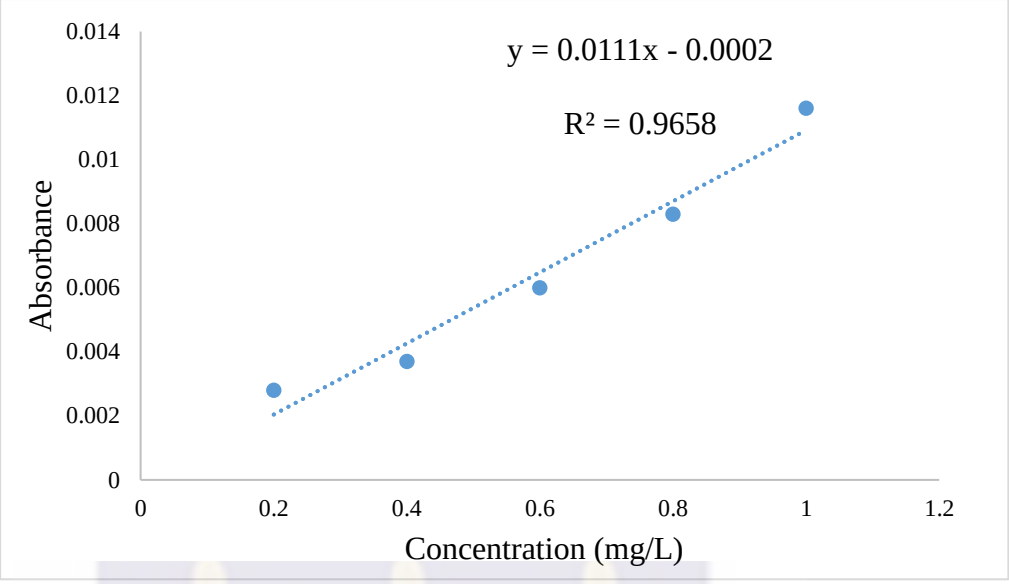

Fig 3.9: Calibration curve for UV spectrometer

3.6 Column Experiment

3.6.1 Collection of Iron-rich Water Samples.

The technique developed was applied on drinking water samples collected from both handmade boreholes (wells) and machine made boreholes within the Ashongman Estates, in the Ga East Municipal of the Greater Accra Region of Ghana.

Fig 3.10: Sampling area in Ashogman Estate (A and B)

Fig 3.11: Water Sampling Kit

Borehole purging was done before sampling to attain a representative sample. It is necessary to remove the stagnant water from the bore casing before a sample is taken, this is called purging. It is recommended that at least three volumes of water be removed and left refill be sampling, this allows the pH, EC and temperature of the ground water to stabilize thereby ensuring that the obtained sample is truly representative of the ground water residing in the aquifer surrounding the borehole"(Borehole purging water watch.org). Sampling was done by putting the water into 350 mL polythene bottles (Fig. 3.11), no chemicals were added to the water, it was sealed and stored in a thermal insulated polyethylene container. 13 sample stations were visited and the water was sampled in duplicate (2 bottles per station). A conductivity meter was used to measure the following parameters for each sample:

The GPS coordinates, total dissolved solutes (TDS), Electro conductivity, Salinity, Temperature, Resistivity and pH these were recorded.

Samples were transported to the laboratories of Ghana Atomic Energy Commission (GAEC) for storage and analysis (Fig. 3.12).

Fig 3.12: Collected water samples in polythene bottles

3.6.2 Application of Developed Iron Removal Technique in Column Experiment.

The samples were taken for initial iron concentration analysis before subjecting them to limestone using the Jenway 6305 UV spectrometer (Fig. 3.13). The batch experiment was not used in the second step but a column method was used this was so as to have a more realistic way of subjecting iron water to limestone as in nature that is no shaking as in the batch methods, limestone samples were weighed using an Mettler AB204-S analytical balance. About 100 g of limestone was weighed and place in each column. After the addition of the limestone to the columns 200 mL of water sample was poured into the columns and the counter was started after about an 1 hour. About 15 mL of the sample was removed from each sample and the reading of the absorbance was collected this reading was converted into concentration with the calibration curve of the UV spectrometer.

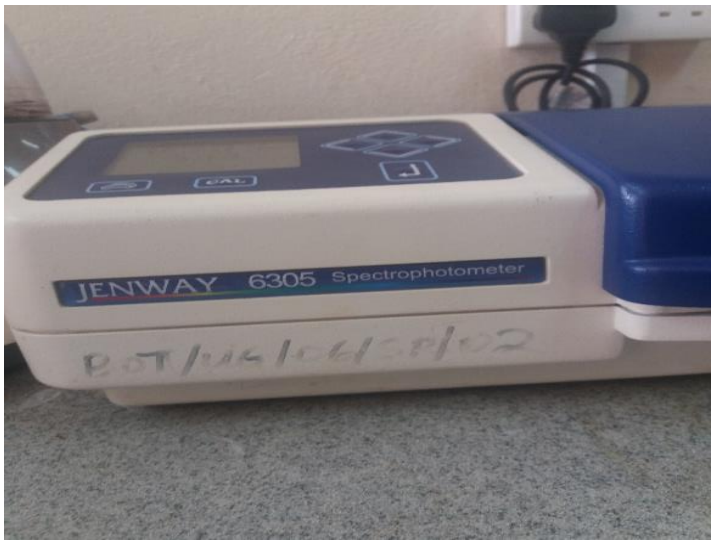

Fig 3.13: UV Spectrophotometer

Analysis of the iron content in various water samples using the UV-Visible spectrophotometer kit (Fig 3.14).

Approximately 10 mL of each water sample was taken after which one FerroVer Iron reagent powder pillow was added respectively. A 5-minute reaction period was allowed for the development of the orange colour for each sample. The initial absorbance of iron in each water sample was measured at wavelength 510 nm from the UV-Visible spectrophotometer. From the calibration curve, the absorbances were extrapolated to find the respective initial iron concentrations in milligram per liter (mg/L) for each water sample.

Fig 3.14: UV Spectrophotometer kit

Four identical columns, of diameter of 9 cm were used, previously the columns were flushed for 10hrs with clear water to wash out grime approximately 200 mL of each water sample was taken and subjected to column packed with 100 grams of limestone respectively. The columns were allowed to stand for one hour to enable maximum interaction between the iron in the various water samples and the limestone (Fig 3.15).

Fig 3.15: Iron Samples in volumetric Separation funnels

The whole rational behind this was to allow the limestone to effectively absorb the iron content in the various water samples.

Fig 3.16: (a) Mounting Iron Samples in volumetric column flasks; (b) Samples in volumetric Separation column flask

After the one-hour reaction period, each column was eluted and the eluate was filtered to get rid of debris of limestone that might have eluted with the water samples (Fig. 3.16 a and b). Approximately 10 mL of each water sample (eluate) was taken after which one FerroVer Iron reagent powder pillow was added respectively. A five minutes reaction period was allowed for the development of the orange color for each sample and the absorbance of iron in each water sample was measured from the UV-Visible spectrophotometer. The respective iron concentrations (mg/L) of each sample was extrapolated from the calibration curve.

The quantity of iron absorbed by the limestone from each water sample was extrapolated from the initial and the final iron concentrations respectively.

3.6.3 Water Standard Tests

Many limits that are required for water to be suitable for drinking (Table 3.3).

Table 3.3: Standards of water tests

Contaminant	Limit
Calcium Carbonate($CaCO_3$) [mg/L]	200
Sulphates (mg/L)	500-1000
Iron (mg/L)	0.3
pH of water	5.5-9.0
Total dissolved Solutes (mg/L)	500-1000
Alkalinity (mg/L)	400

Test for Water Hardness

Water hardness was monitored by the use of water hardness testing kits. The water testing strips after being wet with the sample, changed colour according to the hardness of the water. A colour chart was used to determine the hardness of the sample in ppm (mg/L).

Sulphate Test

Reagents:

- Buffer Solution
- Barium Chloride
- Sulphate Standard
- Conditioning reagent

Procedure

About 20 mL of water sample was added to a 250 mL Erlmenyer flask, followed by the addition of 5 mL of conditioning regent; and thorough mixed by magnetic stirring.

About 1 g of $BaCl_2$ crystals were added and stirring continued till the development of turbid suspensions of barium sulphate ($BaSO_4$). The absorbance of the solution at a wavelength of 420 nm were taken using the UV Spectrophotometer.

For the purpose of calculating the SO_4 content, only maximum value of absorbance was considered.

A blank was prepared for correcting the error due to colour and turbidity, distilled water of equal volume (as that of the diluted volume of original sample) was taken and after adding and mixing 5 mL of conditioning reagent, its absorbance at 420 mn was recorded.

This value was then subtracted from the maximum absorbance value obtained for the original water sample.

The value of absorbance the corresponded to the value of SO_4 concentration obtained from the calibration curve (obtained by the use of sulphate standards) and the concentration of SO_4 in mg per litre was calculated.

Adsorption Percentage and Isotherms

The adsorption percentage was then calculated and results were presented in a chart. The adsorption data were further validated using the model adsorption isotherms by Langmuir (1916) and Freundlich (1909).

3.7 Adsorption Isotherms

The data obtained was validated with Langmuir (1916) and Freundlich (1909) model adsorption isotherms. A graph was made onto which the constants values were evaluated from the intercept and the slope of plot of experimental data Q_e versus (Q_e / C_e) for the Langmuir isotherms and log Q_e vs log C_e for the Freundlich isotherms, Q_e

being the adsorption capacity and C_e the equilibrium concentration of the sample. The adsorption capacity, Q_e (mg/g) of heavy metals can be expressed in the equation (3.11);

$$\boldsymbol{Q_e = \frac{(C_o - C_e) \times V}{m}} \qquad (3.11)$$

C_o and C_e (mg/L) represent heavy metals concentration at initial and equilibrium respectively, m is the mass of limestone adsorbent (g) while the volume is *V*.

The important feature of the Langmuir isotherm is articulated by means of a dimensionless constant denoted as separation factor or equilibrium parameter R_L which is calculated using the equation

$$\boldsymbol{R_L = \frac{1}{1 + K_L C_o}} \qquad (3.12)$$

Where, K_L -Langmuir adsorption constant related to the free energy adsorption (L/mg)

C_o- The highest initial adsorbate concentration (mg/L).

The value of separation factor R_L indicates the adsorption process (Table 3.4):

Table 3.4: Data showing Ranges of RL and their meaning

$\boldsymbol{R_L}$	**Meaning**
(R_L >1)	Unfavorable
(R_L =1)	Linear
(0< R_L <1)	Favorable
(R_L = 0)	Irreversible

For the Freundlich Isotherm,

Taking logarithms on both sides of Freundlich equation (3.13), results in;

$$\boldsymbol{log \frac{w}{m} = logk + logC_e} \qquad 3.13$$

Which is an equation for a straight line. A plot of log (w/m) (Q_e) against log (C_e) results a straight line with slope $1/n$ and intercept log k.

The R^2 value and the straight line obtained after the plot of a graph determines the validity of the Freundlich Isotherm. R^2 is used the determine correlation between the values.

'Most of adsorption studies use these concepts for the adsorption isotherms, which depend on the comparison between the adsorption capacities of different adsorbents in order to evaluate the efficiency of these adsorbents (Sabino De Gisi 2016).

CHAPTER FOUR

RESULTS AND DISCUSSION

The results obtained from the experiments undertaken are presented in the form of Tables and Figures in this Chapter. The results are also discussed.

4.1 Composition of Limestone

The results for the elements composition/mineralogical composition of limestone conducted at the Linear Accelerator Centre, Ghana Atomic Energy Commission are presented in Table 4.1.

For effective removal of excess iron in water, limestone with a high calcium content is required (Akbar, 2016).

The calcium carbonate in limestone increases the pH levels at which iron becomes insoluble and precipitates to form a metal carbonate (siderite); based on this limestone with high calcium should be used for removal of iron in water (Akbar,2015).

Based on the results obtained (Table 4.1) it was concluded that limestone EKLR02 was suitable as compared to EKLD01 due to the fact that the calcium content was high (56.14%) as compared to EKLD01(25.31%),the percentage of iron was low (0.528%) as compared to EKLD01 (2.40%). It was equally very important to note the amount of iron present in the limestone samples as compared to calcium, the least iron percentage was considered because a higher percentage of iron would add more iron to the water being tested and therefore would not be suitable (Akbar,2015).

EKLR02 had less contaminants as zinc, tritium, potassium and manganese were found in trace amounts in EKLR02 compared to EKLD01 (Table 4.1).

Table 4.1: Table showing Elemental composition and percentage of limestone samples

Element	EKLD01		EKLR02	
	Conc. (mg/kg)	% Composition	Conc. (mg/kg)	% Composition
Silicon(Si)	267566	26.76	91911.4	9.19
Iron(Fe)	24030.1	2.40	5276.8	0.53
Calcium(Ca)	253063	25.31	561398	56.14
Potassium(K)	27271.4	2.73	4288.8	0.43
Manganese(Mn)	591.9	0.06	528.2	0.05
Chromium (Cr)	101	0.01	Nil	Nil
Titanium(Ti)	2934.5	0.29	695	0.07
Sulphur(S)	Nil	Nil	189.7	0.02
Zinc(Zn)	Nil	Nil	127.6	0.01

4.2 Radiological safety of limestone samples

Results for the assessment of the radiological safety of limestone samples are presented in Table 4.2. Two grain sizes for the limestone were analysed, G1 and G3 (the largest and least grain sizes). Both samples EKLOR1 and EKLOR2 showed that the ^{40}K concentration was higher than ^{232}Th and ^{238}U. The average concentrations of ^{40}K, ^{232}Th and ^{238}U in soils worldwide in kg/Bq are 420, 45 and 33 respectively (UNSCEAR 2000).

Table 4.2: Radiological activity

Radionulide	Activity (Bq/kg)			
	EKLD01	EKLD01	EKLR02	EKLR02
^{238}U.	90 ± 9.0	61.6 ± 6.2	0.0 ± 0.0	12.5 ± 1.2
^{232} Th	7.1 ± 3.3	17.5 ± 12.5	22.6 ± 1.1	20.8 ± 1.8
^{40}K	220 ± 25	197.8 ±22.4	265.1 ± 27.2	211.9± 20.5

From the mean of results of each sample it was noted that EKLD01 had very high concentration of Uranium (90±9.0 Bq/kg) as compared to the world-wide recommended average values (33 Bq/kg) according to UNSCEAR. However, ^{232}Th and ^{40}K were below the recommended values (90-1,400 Bq/kg for Potassium and 8-80 Bq/kg for Thorium), and in sample EKLR02 all the radionuclides in were below recommended values. Sample EKLR02 contained more thorium than sample EKLD01.

The calculated Annual Effective dose (AED) of the samples was approximately 0.2 mSv/yr for both samples. These values were lower than the recommended 0.40 mSv/yr According to UNSCEAR, 2000.

4.3 Results of Batch Experiment

After the batch setup was done and samples were subjected to limestone for one hour and let to settle for 20 minutes the results of the solution were determined as follows as per parameter measured;

4.3.1 Sample Size Analysis

Both EKLR02 and EKLD01 and were analysed within an hour interval (Table 4.3). After one hour of the experiment and 20 minutes settling (for each experiment), it was noticed that the limestone samples changed colour from their original colour (EKLD01-grey and EKLR02-red) to having a brownish red surface visually signifying that Fe had been adsorbed to the surface and removed from the solution. At this point, the water samples were filtered using Grade 2 Whatman 11 µm filter paper. The filtrate was analysed to determine the of final Iron concentration. It was observed that the limestone with the least grain size (500-1000) µm had adsorbed up-to 98.31% of iron present in the 10 mg/L standard, (Table 4.4).

Table 4.3: Parameters used in batch experiments for the variation of sample size.

ID	Beaker			Blank
	1	2	3	
Mass of limestone (g)	50	50	50	50
pH	6.48	7.31	7.38	7.06
Concentration of iron (mg/L)	10	10	10	0
Size of limestone(µm)	2000-6350	1000-2000	500-1000	500- 1000
Time shaken (min)	60	60	60	60
Volume of water (mL)	200	200	200	200

The percentage removal, R (%) was calculated using the Equation below;

$$R\ (\%) = \frac{C_o - C_e}{C_o} \times 100 \qquad (4.1)$$

Where, C_o and C_e (mg/L) represent iron concentration at initial and equilibrium respectively.

.**Table 4.4**: Average iron percentage adsorption of each limestone sample based on

Parameter	Limestone Sample					
	EKD01			EKLR02		
	1	2	3	1	2	3
Initial concentration (mg/L)	10	10	10	10	10	10
Final concentration (mg/L)	5.755	2.463	1.28	1.454	0.677	0.169
Adsorption percentage (%)	42.45	75.37	87.2	85.46	93.23	98.31

4.3.2 Adsorbent Dosage Analysis

The following results was obtained for the investigated adsorbent dose.

Table 4.5: Parameters used in batch experiments for the variation of sample dosage.

Parameter	Limestone Sample					
	EKLDO1			EKLRO2		
	1	2	3	1	2	3
Mass of limestone (g)	20	50	100	20	50	100
pH(iron standard)	6.48	7.31	7.38	6.48	7.31	7.38
Concentration of iron (mg/L)	10	10	10	10	10	10
Size of limestone (µm)	500-1000	500-1000	500-1000	500-1000	500-1000	500-1000
Time shaken (min)	60	60	60	60	60	60
Volume of water (mL)	200	200	200	200	200	200

Iron removal efficiency escalates with increasing dose of limestone (Table 4.5). This was due to a large surface area for adsorption with many binding sites for 100 g doses as compared to lower ones (Aziz,2004). Removal efficiency (adsorption) was greater when limestone was 100 g. The 100 g mass limestone adsorbed significantly compared to the 20 g and 50 g doses of limestone.

It was observed that for EKLR02 with 20 g of the limestone only about 60% of iron had been adsorbed; the 50 g limestone adsorbed about 80%, while the 100 g limestone adsorbed 93% of the iron in the drinking water as shown in Fig 4.1;

EKLR02

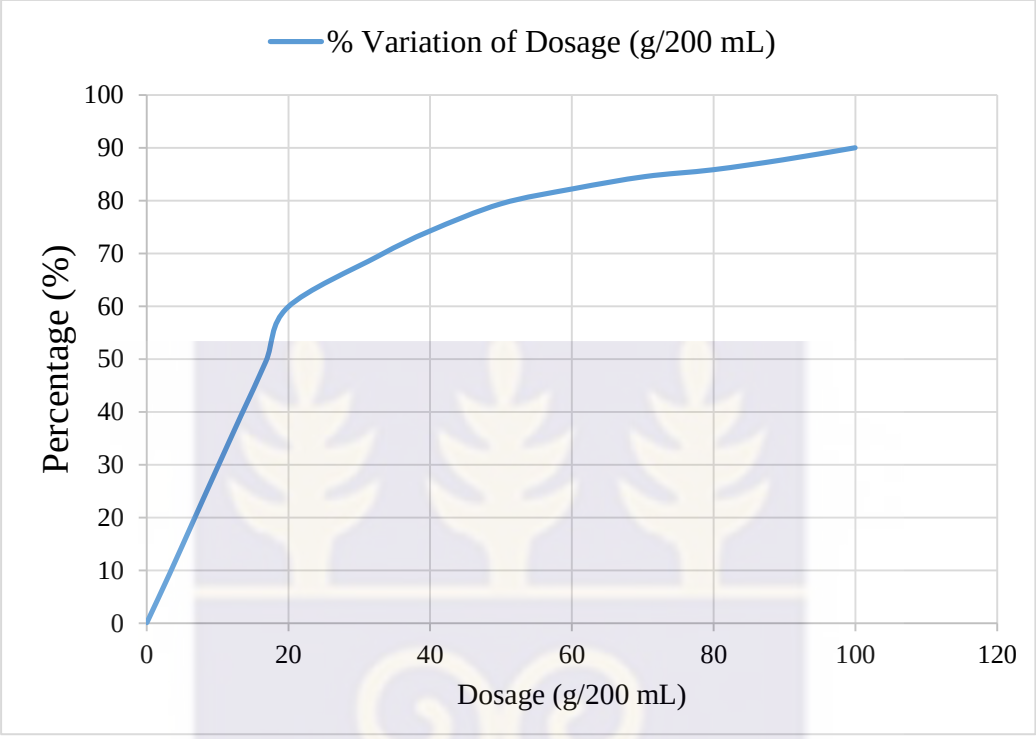

Fig 4.1: Plot of limestone sample dosage (g/200 mL) against percentage adsorption (%)

For sample EKLD01 it was observed that it had the most adsorption (80%) take place with 100 g as compared to the 20 g and 50 g doses just as EKLOR2.

It was also observed that with 20 g of limestone, only 43.6 % of iron was adsorbed; 50 g limestone adsorbed about 70 %, while with 100 g limestone adsorbed 80 % was obtained (Fig 4.2).

EKLD01

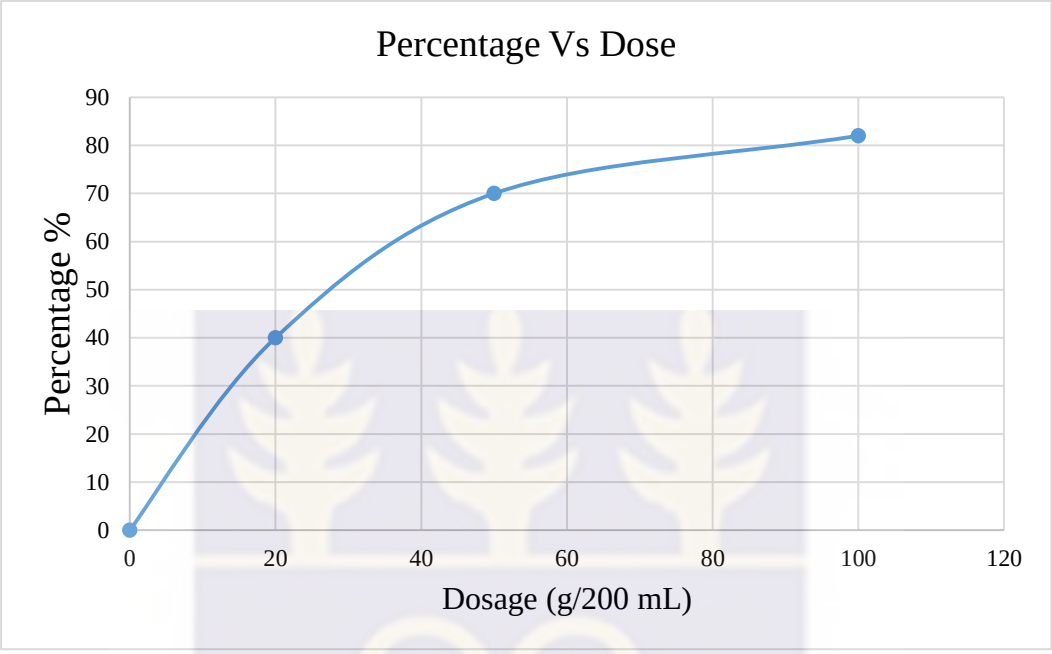

Fig 4.2: Plot of limestone sample dosage (g/200ml) against percentage adsorption (%)

At optimum dosage, equilibrium was attained when the rate of sorption was the same as the rate of desorption (Akbar, 2016). Increasing the quantity of limestone increased the percentage removal of iron in the drinking water.

From the results obtained, the maximum adsorption dosage was at 100 g/200 mL and the highest adsorption with limestone sample EKLOR2.

4.3.3 Contact Time (Residence Time)

The influence of interaction time on adsorption of iron was studied. Only one limestone sample was used with reference to the previous experiments conducted (sample size and dosage), leading to the choice of EKLOR02 as the suitable limestone for the removal of iron from the drinking water.

The residence time varied between 60 minutes, 90 minutes and 120 minutes. Maximum rate of removal occurred within the first 60 minutes, at 90th minutes the rate of adsorption had decreased and at 120 minutes there was no drastic change in the limestone removal which established that the system has reached the equilibrium point and the adsorption rate had reached its maximum (Fig 4.3). All the reaction sites had probably been bound to and no further reaction could take place.

Effect of Contact time

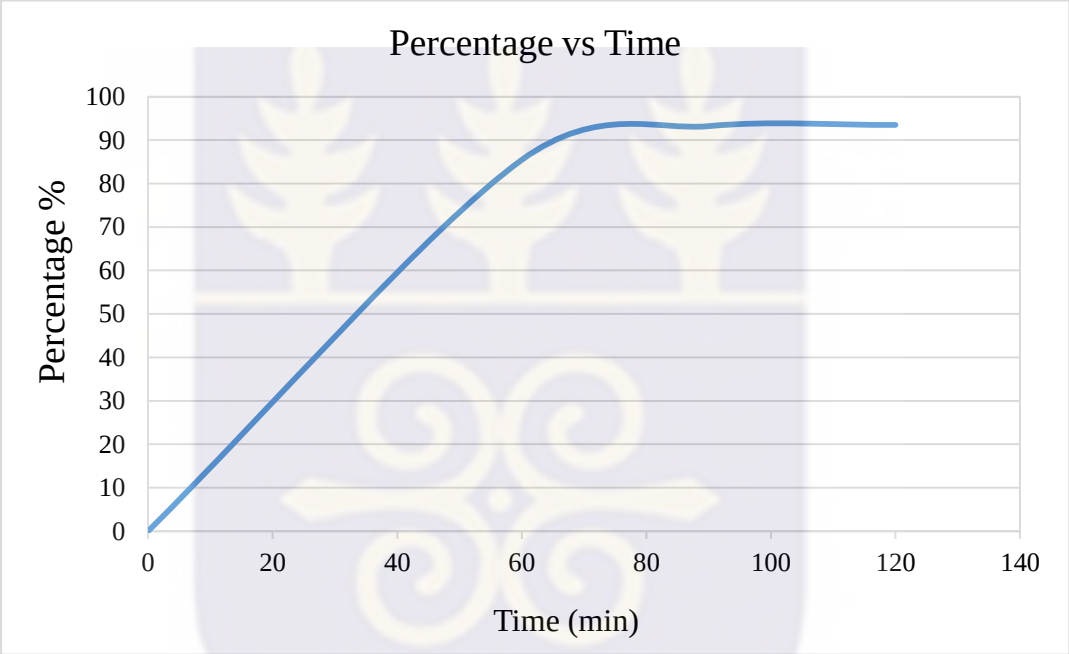

Fig 4.3: Plot of contact time against percentage adsorption (%)

From Fig 4.3, the optimum adsorption occurred at the 90th minute. Drastic change in adsorption occurred in between the 60th and 90th minutes.

4.3.4 pH

The effect of pH was assessed. After observation it was noted that a change in pH caused the adsorption of iron being more at a greater pH (pH 7-14) as compared to when it was at a lower pH (1-5), this was as a result of limestone decomposing at lower

pH to calcium metal and adsorption would not take place (Fig. 4.4). It was observed that increasing the pH levels resulted in greater adsorption as a result of iron becoming insoluble enabling precipitation and adsorption to form a metal carbonate (siderite) [Akbar,2013].

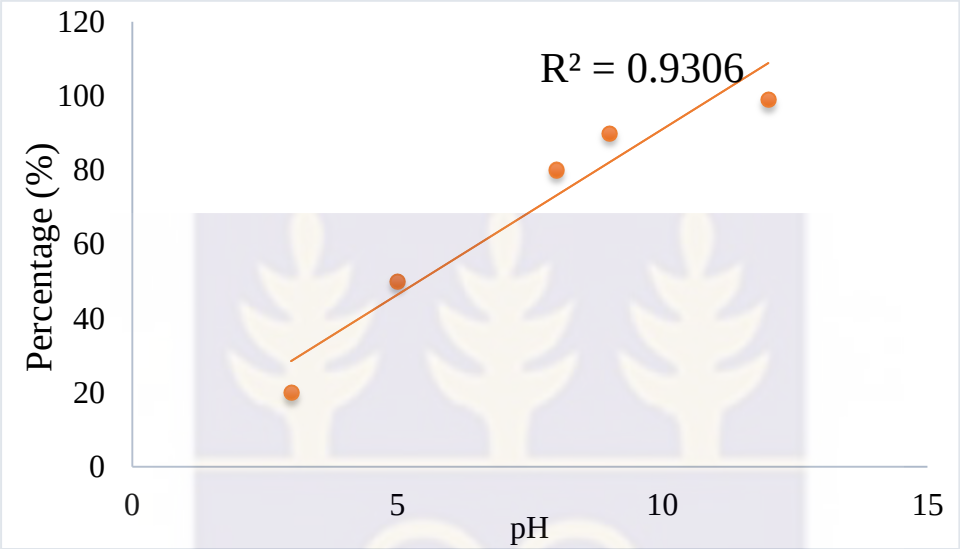

Fig 4.4: Plot of pH against percentage adsorption (%)

4.4 Results of Application of Developed Technique on Real Samples (Column Experiment)

The developed analytical technique was used to analyse real samples collected from the Ashongman Estates in the Ga East Municipal (about 10 km from the Ghana Atomic Energy Commission premises and about 9.6 km from Abokobi, the capital of the Ga East Municipal). The results of the physico-chemical parameters of the sampled water are presented in Table 4.6.

Table 4.6: Results of application of developed technique on real samples (Column Experiment)

Sample ID	Geographical Coordinates of sample locations			Physico-Chemical parameters						
	longitude (˚S)	Latitude (˚N)	Elevation	pH	Temp (˚C)	Electrical Conductivty (µsv/cm)	Salinity (psu)	Total Dissolved Solids (mg/L)	Resistivity (Ωcm)	Alkalinity (mg/L)
AS02	0.23468	5.68217	68	6.47	29.9	1207	0.6	604	827	740
AS03	0.33373	5.68284	61	6.86	30.1	1164	0.5	582	858	1159
AS04	0.23474	5.70237	98	6.47	29.1	456	0.1	228	2.2	520
AS05	0.23319	5.70237	93	4.15	30.2	213	0	107	4.7	56
AS06	0.23104	5.70284	82	5.7	29.6	371	0.1	186	2.69	316
AS07	0.23049	5.70236	83	5.42	29.2	334	0.1	167	3	134
AS08	0.22911	5.70221	79	7.6	28.2	1062	0.1	531	2.86	3120
AS09	0.23064	5.70307	80	5.96	29.6	350	0.5	175	942	262
AS10	0.23088	5.70373	93	5.18	29.9	267	0	134	3.75	72
AS11BH	0.22994	5.70385	87	6.93	8.8	583	0.2	292	1715	268
AS11BHT	0.22997	5.7038	85	4.72	30.5	600	0.2	300	1668	42
AS12	0.22891	5.70318	77	5.68	31.5	498	0.2	249	2.01	130
AS13	0.22844	5.70208	81	5.24	31.5	518	0.2	259	1935	136

4.4.1 Report of Initial Fe Concentration, Final Fe Concentration, and Percentage Adsorption

4.4.1.1 Iron to Limestone Adsorption Percentage

The absorbance of each water sample collected was read in triplicate and the average was calculated. The final and initial concentrations for each sample were calculated to get the final percentages of iron removal using equation 4.2.

Calculation of Percentage Adsorption

$$\textbf{Adsorption}\ (\%) = \frac{C_i - C_F}{C_o} \times 100 \qquad (4.2)$$

Where,

C_o = Initial concentration (mg/L)

C_f =Final concentration (mg/L)

Data for Fe concentration are presented as the mean for three replicate measurements. It was observed that samples AS13, AS12, AS07, and AS10 had high absorbance as compared to the other samples in all three trials meaning that the iron content in these samples was slightly large as compared to the other samples. (Table 4.7)

From the Table below, it was observed that the highest initial iron concentration in water samples collected was 4.67, which is beyond the recommended WHO standard for iron in drinking water (0.03 mg/L).

Table 4.7: Showing Initial Fe Concentration, Final Fe Concentration, and % Adsorption

Sample ID	**Conc. Of Fe (mg/L)**		**Adsorption (%)**
	Initial	Final	
AS01	0.23	0.20	14.09
AS024	0.25	0.22	10.63
AS03	0.24	0.22	6.07
AS04	0.21	0.20	7.04
AS05	0.31	0.25	20.37
AS06	0.29	0.20	31.58
AS07	1.24	0.20	84.26
AS08	0.23	0.19	16.87
AS09	0.20	0.19	5.23
AS10	0.28	0.23	19.16
AS11BH	0.33	0.28	14.67
AS11BHT	4.67	0.26	94.53
AS12	0.21	0.19	10.71
AS13	1.33	0.21	84.40

All the concentrations were deduced, standard deviations of the results were calculated and the final percentage was calculated. It was noted that the highest percentage removal was 94.53 % while the least removal was 5.23 % this was as a results of different properties of the water that was analysed. The reduction factor could not be exactly the same.

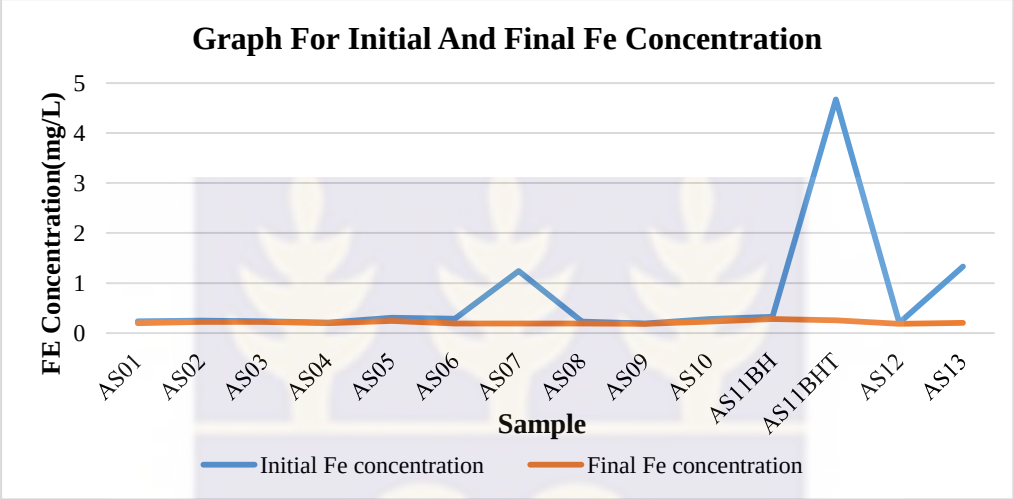

Fig 4.5: Plot of sample ID against iron concentration (Initial and final concentrations).

From each sample as shown;

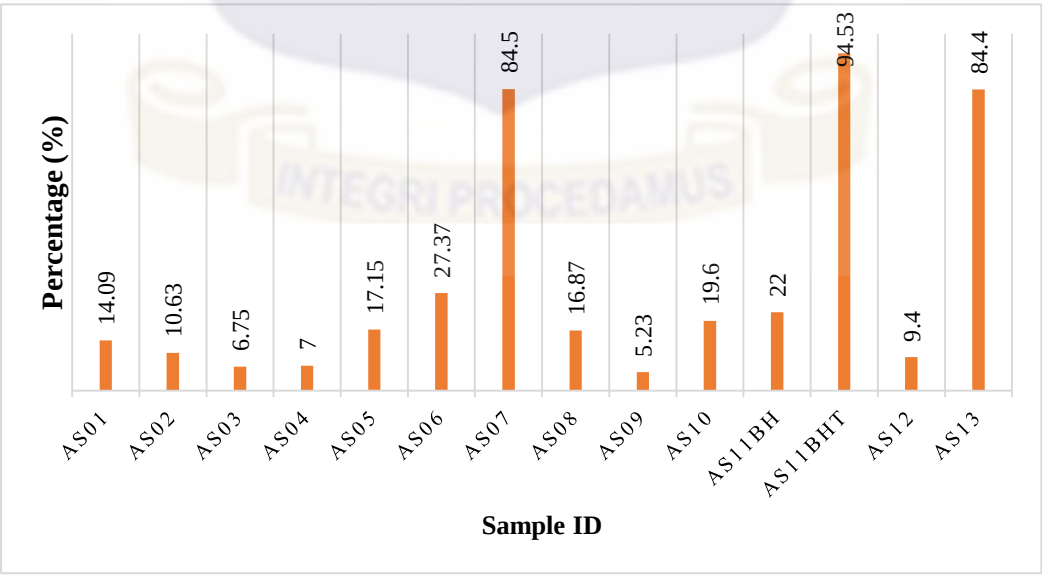

Fig 4.6: Chart of % Adsorption of water samples collected

From Figs. 4.5 and 4.6, it is obvious that samples AS07 and AS13 had significant iron concentration removed from them with AS11BHT being the highest having 94.53 %. The least amount of iron percentage removal was for AS09 in which only 5.23 % of iron had been removed.

The difference in Iron removal of each sample can be attributed to the fact that the water samples having sampled from different areas had different forms of iron present in them e.g. Iron was not in its soluble form. It is impossible to get the same factor for all the water samples collected.

4.5 Water Sufficiency to Be Used For Drinking

After the water samples had been subjected to limestone, they were tested according to the WHO and standards of USA to verify if the water was suitable for drinking i.e. insuring that the technique that was applied to the water samples did not introduce any foreign matter and was considered safe for drinking.

4.6 Recommended Standards for Water Results.

The water samples were tested for various parameters to ensure that the water subjected to the adsorption technique was safe for drinking.

Most of the samples were within the recommended limits, Table 4.8 but it was noticed that same samples had the alkalinity and sulphates beyond the recommended levels, this was attributed to the fact that these samples initially had a high alkalinity and sulphates.

Table 4.8: Recommended Standards for normal drinking water

Sample ID	Water hardness (mg/L)	Total dissolved solutes(mg/L)	Sulphates (mg/L)	pH	Alkalinity (mg/L)
AS01	200	490	555	6.74	603
AS02	134	609	200	6.87	779
AS03	120	590	750	6.36	1142
AS04	70	678	673	6.27	580
AS05	123	658	826	4.95	90
AS06	134	736	943	5.2	407
AS07	180	650	902	5.92	230
AS08	143	321	860	7.1	3320
AS09	104	760	70	5.26	450
AS10	120	549	949	5.98	250
AS11BH	98	697	967	6.33	678
AS11BHT	67	643	624	4.22	78
AS12	79	780	570	5.28	160
AS13	32	505	300	5.94	145
Recommended Values	100-200	>1000	0-250	9-Jul	>1000

4.7 Validation of Adsorption Data using the Langmuir and Freundlich Adsorption Isotherm

4.7.1 Langmuir Adsorption Isotherm

The adsorption data (Column Experiment) obtained from the studies ware validated using model Adsorption Isotherms by Langmuir (1916) and Freundlich (1909). The plots are presented in Fig 4.8 (Langmuir) and Fig 4.9 (Freundlich). The calculation of the parameters needed for the concentration of the Plots that is Adsorption capacity (Q_e), Equilibrium Concentration (C_e) and the ratio Qe/ C_e are presented in Table 4.9

Table 4.9: Langmuir results of column experiment data showing Adsorption Capacity,

SAMPLE NO.	Q_e (Adsorption capacity mg/g)	Ce (equilibrium concentration)	Q_e/C_e
AS01	3.3×10^{-5}	0.2012	1.64×10^{-4}
AS02	2.65×10^{-5}	0.2227	1.19×10^{-4}
AS03	1.44×10^{-5}	0.2228	6.45×10^{-5}
AS04	1.5×10^{-5}	0.1982	7.56×10^{-5}
AS05	6.3×10^{-5}	0.2463	2.56×10^{-5}
AS06	9.01×10^{-5}	0.1952	4.61×10^{-4}
AS07	1.05×10^{-5}	0.1952	5.35×10^{-3}
AS08	3.9×10^{-5}	0.1922	2.03×10^{-4}
AS09	1.02×10^{-5}	0.1850	5.51×10^{-5}
AS10	5.4×10^{-5}	0.2282	2.37×10^{-4}
AS11BH	4.8×10^{-5}	0.2793	1.71×10^{-4}
AS11BHT	4.41×10^{-3}	0.2553	0.01779
A41S12	2.22×10^{-5}	0.1850	1.2×10^{-4}
AS13	1.12×10^{-3}	0.2075	5.41×10^{-3}

Where Q_e is the adsorption capacity and C_e is the equilibrium concentration**.**

Langmuir Graph of Q_e (Adsorption Capacity Vs Q_e/C_e)

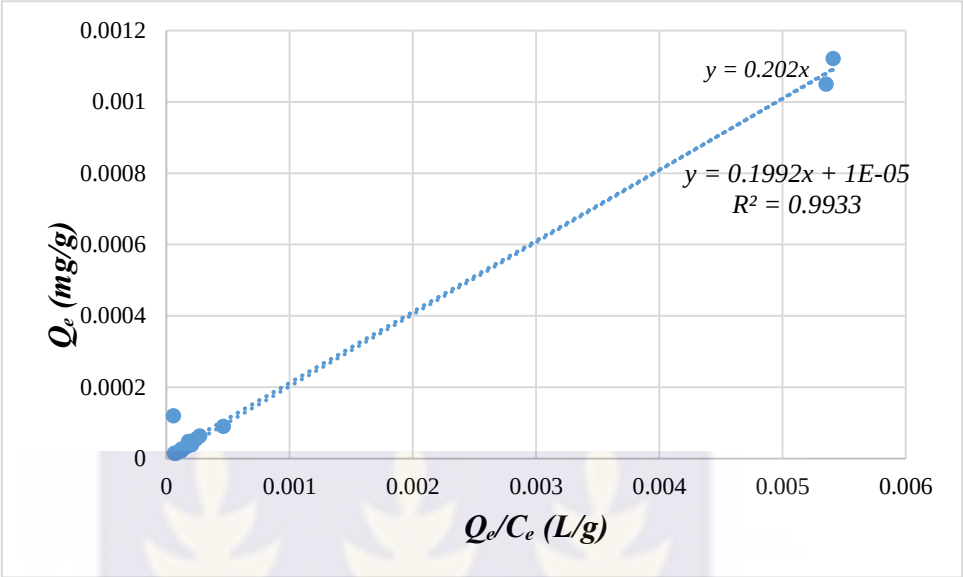

Fig 4.7: Plot of Adsorption data on the Langmuir Isotherm model

The slope of the linear plot of experimental data of Q_e versus (Q_e / C_e) [Fig 4.7] has a very strong R^2 correlation of 0.9933. This shows that the value was close to one.

The maximum adsorption capacity of the iron was found from the equation together with the K_L constant.

The y intercept equation for the graph plotted (linear plot) [Fig 4.8] was found to be;

$$y = 0.202\ x$$

$$\boldsymbol{Q_e} \text{ vs } \frac{\boldsymbol{Q_e}}{\boldsymbol{C_e}} \rightarrow \text{plot}$$

To find the constant the equation of plot use is;

$$\boldsymbol{Q_e} = -\frac{\boldsymbol{1}}{\boldsymbol{K_L}}\frac{\boldsymbol{q_e}}{\boldsymbol{C_e}} + \boldsymbol{Q_{max}} \qquad (4.3)$$

This equation is a plot for a straight line;

$$\boldsymbol{y = mx + c} \qquad (4.4)$$

$y = Q_e$; $mx = -\frac{1}{K_L}\frac{Q_e}{C_e}$ and $c = Q_{max}$

Equating the constants K_L and Q_{max} to the graph linear equation (4.5) gradient and intercept respectively;

$$y = 0.199\,x + 1 \times 10^{-5} \quad (4.5)$$

$$\therefore\ Q_{max} = 1 \times 10^{-5} \quad (4.6)$$

While K_L can be calculated from equation (4.3) as follows;

$$\boldsymbol{Q_e = -\frac{1}{K_L}\frac{q_e}{C_e} + Q_{max}} \quad (4.3)$$

$$\boldsymbol{K_L} = -\frac{1}{0.199} \quad (4.3)$$

$\therefore \boldsymbol{K_L}$= -5.025.

The separation factor $\boldsymbol{R_L}$ is calculated with the formula below;

$$\boldsymbol{R_L = \frac{1}{1 + K_L C_o}} \quad (4.4)$$

Where $\boldsymbol{R_L}$ ***is*** the separation factor

K_L is constant, and

C_o is the initial highest concentration (mg/L)

$$\boldsymbol{R_L} = \frac{1}{1+(-5.025 \times 1.3303)}$$

Although R_L < 1, the results showed that the obtained data did not agree with the Langmuir isotherms in no case should the result of the separation factor produced be <0 or negative in such an instance it is an indication that the data obtained did not agree with Langmuir and the adsorption that occurred was not unimolecular.

Scatchard linearization of the Langmuir model (Type 4), the variables Q_e and Q_e/C_e are not independent in the Type 4 linearization. In this case the correlation between Q_e and Q_e/C_e is underestimated, the equation provides poor fit to the data that do not conform to the Langmuir model as seen from the results and the calculation made for R_L (Hai et al., 2017).

From the data, it was observed that concentrations that had been greater than one had the highest adsorption capacity (more than 50% adsorption as compared to other samples).

The Langmuir isotherms were used on the three samples that had concentrations above 1 mg/L (1 ppm) and it was observed that the graph agreed with the Langmuir isotherm.

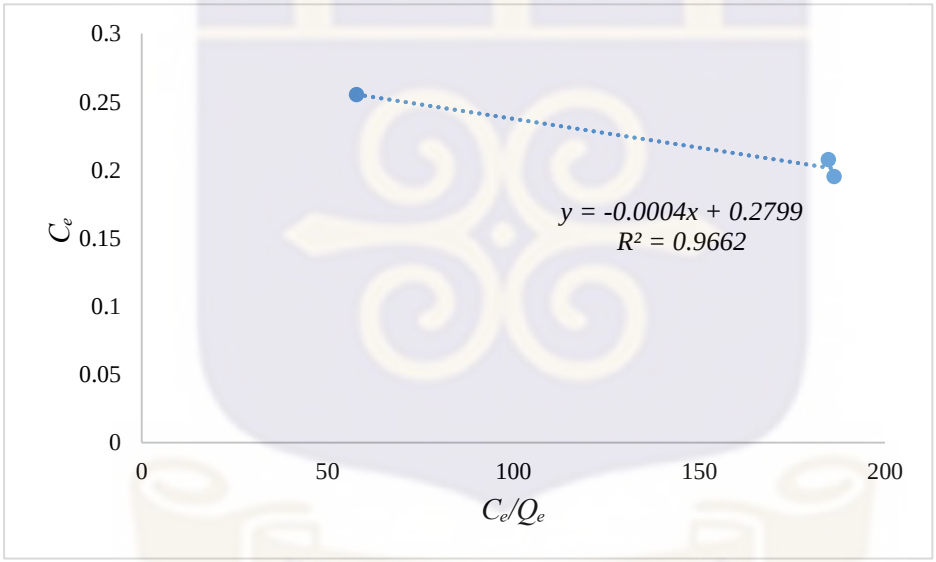

Fig 4.8: Plot of Adsorption data on the Langmuir Isotherm model

The R_L value of 1.02, which form the three conditions for the R_L suggests that the data points were linear and they followed the Langmuir isotherm. This showed that the limestone adsorption technique followed the Langmuir Isotherm only if the concentrations of iron was above 1mg/L. This can also indicate that the limestone adsorption technique is effective with high iron concentrations.

4.7.2 Freundlich Results

The Freundlich graph was plotted which corresponds to the equation;

$$log\frac{w}{m} = logk_f + \frac{1}{n} logC_e \qquad (4.6)$$

Where, $q_e = \frac{w}{m}$, equilibrium adsorption capacity (L/g)

n and k_f *are Freundlich constants*

C_e *is equilibrium concentration (m/g)*

The graph was plotted as log Q_e vs $logC_e$ (Fig. 4.9)

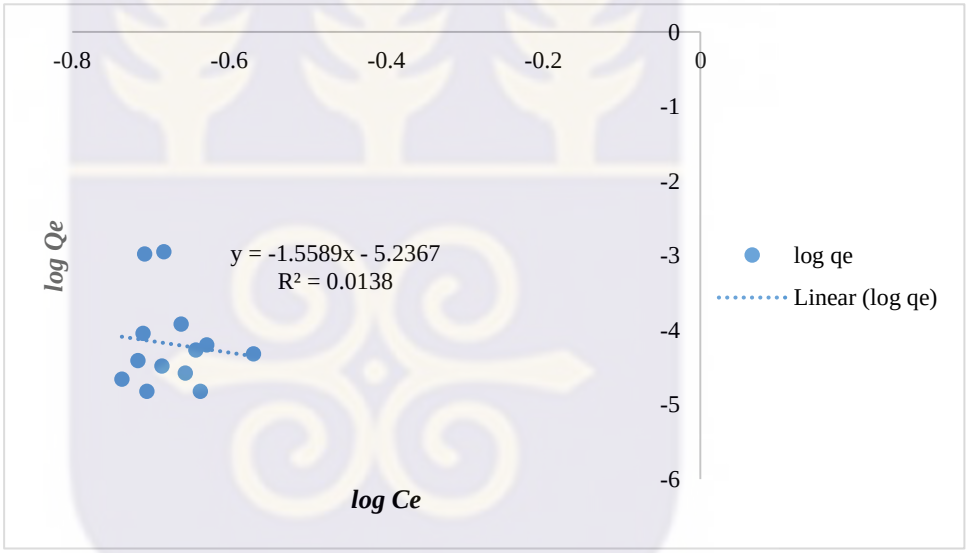

Fig 4.9: Plot of Adsorption data on the Freundlich Isotherm model

The plot of log C_e vs log Q_e did not give a straight line; and the correlation coefficient, R^2, was 0.0138. The weak correlation indicated that the adsorption data did not agree or fit into the Freundlich Adsorption Isotherm model.

The equation of the graph was

$$y = -1.5589x - 5.2367 \qquad (4.6)$$

From equation (4.5), constants k_f and n can be calculated using the linear graph equation (4.6) and equating the linear equation variables;

$$y = mx + c \qquad (4.7)$$

$$\therefore \quad y = \log \frac{w}{m} \quad ; \quad mx = \frac{1}{n} \log C_e \quad and \quad c = \log K_f$$

Using equation (4.6),

$$-1.5589 = \frac{1}{n} \qquad \therefore n = -0.6414$$

$$-5.2367 = \log k_f \qquad \therefore k_f = 5.8 \times 10^{-6}$$

From the results obtained it was observed that the data did not agree with the Freundlich models the values of the R^2 was not close to 1(0.0138) which showed there was no correlation between the points. The K_f constant was negative (-5.2367).This is due to the low concentrations that were obtained after the technique and the fact that the samples did not have a uniform separation factor.

CHAPTER FIVE

CONCLUSION AND RECOMMENDATION

The study had revealed that limestone is effective for the removal of iron in ground water and drinking water, therefore suitable alternative for the removal of heavy metals like iron from ground water.

5.1 Limestone Composition and Batch Experiments

From the results it was seen that EKLR02 was the best suitable limestone sample for this technique, it had the highest amount of calcium on it (56.14%), it had less impurities with its iron content (0.528%) being minimal resulting in no interference with the results.

Adsorption occurred in all the batch experiments. The sample size (grain size) was found to work best at 500-1000 µm, 98% iron removal was observed at this grain size as opposed to the other two sizes with 1000-2000 µm and 2000-6300. Optimum dosage was found to be 100g/200 mL, at this dosage 93% adsorption occurred. The study also revealed that the higher the dosage the more adsorption that took place. However, after 100 g there was no drastic change in the adsorption indicating that adsorption had reached its optimum.

Similarly, it was observed that changes in pH led to corresponding changes in adsorption (that is an increase in pH led to a corresponding increase in adsorption). This may be attributed to iron ions (Fe^{2+}) becoming insoluble and precipitating to form a metal iron at high pH (7-14) as opposed to low pH (1-5).

Additionally, it was observed that the adsorption increased with time; with drastic adsorption change noticed between 0 and 60 minutes. After 60 minutes the adsorption remained constant despite change in time.

5.2 Radiological safety

From the average activity concentration obtained it was observed that for the purposes of using the limestone samples (EKLR02 and EKLD01) in the removal of iron in drinking water, EKLR02 was the most suitable limestone sample due to its low Uranium (^{238}U) concentration. Considering the high solubility of Uranium in water which could led to toxicity related problems in humans. It was observed that EKLRO2 had a higher concentration of ^{232}Th as compared to EKLDO1, but despite the concentration of Thorium being high it could be easily removed from water due to thorium being insoluble in water. Thorium precipitates with particulate in water and easily removed by filtration. Both samples were relatively radiologically safe because they did not exceed the recommended calculated mean annual effective dose of 0.4 mSv/yr according to UNSCEAR, (2000)

5.2 Column Adsorption Experiments

The method developed was applied in Column adsorption experiments on real water samples from Ashogman Estates, Ga East Municipal of the Greater Accra Region of Ghana. The observed highest percentage adsorption was 94.53% and the lowest adsorption was 5.23 %. However the observed adsorption for the water samples were not uniform or consistent due to the different physico-chemical properties (pH, TDS, Salinity, to mention a few) of the water samples as they were obtained from different places. Due to differences in the interaction of water with the limestone, adsorption could not take place at the same rate. It was observed that water samples with iron concentrations above 1 mg/L had the highest adsorption. This can be attributed to the fact that the limestone may have worked well or adsorbed high Iron concentration better than low Iron concentration. It was observed that after subjection of water samples to

the limestone the colour of the water partly changed to cloudy this could be avoided by the discolouration of the limestone before using it in the technique.

5.3 Adsorption Isotherms

The Model Adsorption Isotherms by Langmuir (1916) and Freundlich (1909) did not adequately describe the adsorption data obtained. It however, did show that the samples that had initial Fe concentrations above 1 mg/L did have a linear relationship between the amount of adsorbent used and the concentration of the adsorbate.

5.5 Recommendation

i. There must be discoloration of the limestone sample before its use as it was observed that during the experiment water samples assumed the colour of the limestone. Activated charcoal is recommended for the discolouration

ii. The efficacy of adsorption was not effective in water samples with iron concentration less than 1 mg/L. There is a need for further study to assess the effect of iron concentration on limestone in the developed technique.

iii. The outcome from the adsorption isotherms requires that different techniques be used in analysing the adsorption efficiency such as adsorption thermodynamics and adsorption kinetics, where the data fails to obey Langmuir (1916) and Freundlich (1909).

iv. In future experiments the radiological safety of the water samples should be determined before and after the experiment.

REFERENCES

Akar, S.T. (2009) "Removal of copper (II) ions from synthetic solution and real wastewater by the combined action of dried Trametes versicolor cells and montmorillonite", *Hydrometallurgy* 06, 98–104.

Akbar N. A**.,** Aziz H A., and Adlan M.N. (2015) "Iron and Manganese Removal from Groundwater Using High Quality Limestone", *Applied Mechanics and Materials*, Vol. 802, pp. 460-465,

Aman T., (2011). Principle, working and applications of UV spectroscopy. Retrieved on July 03, 2017. From: http://www.indiastudychannel.com/resources/146681-Principleworking- and-applications-of-UV spectroscopy.aspx

Anspaugh, Lynn R. (1976): "In situ methods for quantifying specific radionuclides." *IEEE Transactions on Nuclear Science* 23.3 1190-1196.

Arthy, M. and Phanikumar, B.R., (2016). Efficacy of iron-based nanoparticles and nanobiocomposites in removal of Cr 3+. *Journal of Hazardous, Toxic, and Radioactive Waste,* 20(3), p.401-605.

Armenante, P.M., Adsorption. NJIT. Retrieved from: http://cpe.njit.edu/dlnotes/CHE685/Cls11-1.pdf. Accessed on: 1st May 2017

Ashok D., and Ferbel T. (2003). *Introduction to nuclear and particle physics*. Singapore. World Scientific.

Aziz, H. A., Adlan, M. N., & Ariffin, K. S. (2008). Heavy metals (Cd, Pb, Zn, Ni, Cu and Cr (III)) removal from water in Malaysia: Post treatment by high quality limestone. *Bioresource technology*, *99*(6), 1578-1583.

Aziz, H. A., Yusoff, M. S., Adlan, M. N., Adnan, N. H., & Alias, S. (2004). Physico-chemical removal of iron from semi-aerobic landfill leachate by limestone filter. *Waste Management*, *24*(4), 353-358.

Ayoob, S., Gupta, A.K. and Bhakat, P.B., (2007). Performance evaluation of modified calcined bauxite in the sorptive removal of arsenic (III) from aqueous environment. Colloids and Surfaces A*: Physicochemical and Engineering Aspects*, 293(1-3), pp.247-254.

Badmus, M. A. and Audu, T. O. (2009). Periwinkle shell: Based granular activated carbon for treatment of chemical oxygen demand (COD) in industrial wastewater. *Can. J. Chem. Eng.,* 87: 69-77. doi:10.1002/cjce.20140

Colter A., and Robert Louis M, (2006). *Iron in drinking water*. Moscow: University of Idaho.

Egbok, C.E G.I. Nwankwor, I.P. Orajaka and A.O. Ejiofor,(1989). Principles and Problems of Environmental Pollution of Groundwater Resources with Case Examples from Developing Countries. *Environmental Health Perspectives*, 83: 39-68.

Dąbrowski A. (2001). Adsorption - from theory to practice. Advances in Colloid and *Interface Science*. 93(1/3), 135-224.

Devi R.R., Iohborlang M. U., Bodhaditya D., Kusum B., Ashim J.T., Prasanta K. R., Saumen B.,and Lokendra S. (2014). "Removal of iron and arsenic (III) from drinking water using iron oxide-coated sand and limestone." *Applied Water Science* 4(2), 175-182.

Do D.D., (1998). Adsorption analysis: equilibria and kinetics London: *Imperial College Press*. Vol. 2, pp. 1-18.

Dobbs A.J., (2011). Particle rate and host accelerator beam loss on the MICE experiment. No. FERMILAB-THESIS--2011-51; MICE-THESIS--2011-DOBBS.

Doyi I., Oppon, O.C., Glover E.T., Gbeddy G. and Kokroko W., (2013). Assessment of occupational radiation exposure in underground artisanal gold mines in Tongo, Upper East Region of Ghana. *Journal of Environmental Radioactivity*, 126, 77-82.

Darko E. O., Tetteh G. K., Akaho E. H. K. (2005). Occupational radiation exposure to norms in a gold mine, *Radiation Protection Dosimetry*, 114(4), 538–545.

Elinder C-G. Iron. In: Friberg L, Nordberg GF, Vouk VB, eds. (1986) Handbook on the toxicology of metals, Vol. II. Amsterdam, *Elsevier*. Pages 276-297.

El-Taher A., Uosif M. A. M., Orabi A. A. (2007). Natural radioactivity levels and radiation hazard indices in granite from Aswan to Wadi El-Allaqi southeastern desert, Egypt, *Radiation Protection Dosimetry*, 124(2),148–154.

Faanu A., Kpeglo D.O., Sackey M., Darko, E.O., Emi-Reynolds G., Lawluvi H., Awudu R., Adukpo O.K., Kansaana C., Ali, I.D. and Agyeman B., (2013). Natural and artificial radioactivity distribution in soil, rock and water of the Central Ashanti Gold Mine, Ghana. *Environmental Earth Sciences*, 70(4), 1593-1604.

Fawzia Z. Y.M., and Wahab M.A.E. (2009). "External exposure due to natural radioactivity in some household kits." *International Journal of Low Radiation* 6.1, 8-20.

FNAL (Fermi National Accelerator Laboratory), Batavia, IL (United States), (2011). Retrieved from Historical information from the Fermilab History and Archives Project website (https://history.fnal.gov/).

Ferreira S.L.C., Andrade H.M.C., Talma Hilda C.S. (2004)."Characterization and determination of the thermodynamic and kinetic properties of the adsorption of the molybdenum (VI)-calamite complex onto active carbon", *Journal of Colloid and Interface Science*, 270, 276–280.

Fookes, P. G., and Hawkins A. B. (1988). "Limestone weathering: its engineering significance and a proposed classification scheme." *Quarterly Journal of Engineering Geology and Hydrogeology* 21.1: 7-31.

Gao S., Sun R., Wei Z., Zhao H., Li H., Hu F**.** (2009). Size-dependent deflourization properties of sysnthetic hydroxyapatite. *Journal of Fluorine Chemistry*, 130, 550-556

Giles C. H., Smith D., Huitson A., (1974). A general treatment and classification of the solute adsorption isotherm. I. Theoretical. *Colloid and Interface Science*.47, 755-765.

Girods P., Dufour A., Fierro V., Rogaume Y., Rogaume C., Zoulalian A., Celzard A., (2009). Activated carbons prepared from wood particleboard wastes: Characterisation and phenol adsorption capacities, *Journal of Hazardous Materials*, 166(1), Pages 491-501.

Gunnar F.N., Bruce A.F. and Monica N., (2015). Preface, In Handbook on the Toxicology of Metals (Fourth Edition), Academic Press, San Diego, Pages v-vi, ISBN 9780444594532.

Gupta VK, Saini VK, Jain N. (2005). Adsorption of As (III) from aqueous solutions by iron oxide-coated sand. *J Colloid Interface Sci*. 288(1), 55–60.

Gupta V.K., (1998). "Equilibrium uptake, sorption dynamics, process development, and column operations for the removal of copper and nickel from aqueous solution and wastewater using activated slag, a low-cost adsorbent." *Industrial & Engineering Chemistry Research* 37(1), 192-202.

Glynn P.D. and L.N. Plummer (2005), ‘‘Geochemistry and the understanding of ground-water systems,’’ *Hydrogeology Journal*, 13 (1), 263–287.

Hall K. R., Eagleton, L. C., Acrivos, A. and Vermeulen, T. (1966) Pore and solid-diffusion kinetics in fixed-bed adsorption under constant-pattern conditions. *Industrial &. Engineering Chemistry Fundamentals*, 5(2), 212-222.

Hamdaoui O., and Naffrechoux, E. (2007). Modeling of adsorption isotherms of phenol and chlorophenols onto granular activated carbon: Part I. Two-parameter models and equations allowing determination of thermodynamic parameters. *Journal of Hazardous Materials.* 147(1-2), 381-394.

Hashem A., Abou-Okeil, A., El-Shafie, A. and El-Sakhawy, M., (2006). Grafting of high α-cellulose pulp extracted from sunflower stalks for removal of Hg (II) from aqueous solution. *Polymer-Plastics Technology and Engineering*, 45(1), 135-141.

ISO (International Organization for Standardization) (1988). ISO 6332:1988-Water Quality-Determination of Iron, Geneva, Switzerland, pp.301-310.

Jibiri, N.N., Isinkaye, M.O., Bello, I.A. and Olaniyi, P.G., (2016). Dose assessments from the measured radioactivity in soil, rock, clay, sediment and food crop samples of an elevated radiation area in south-western Nigeria. *Environmental Earth Sciences*, *75*(2), 107.

Jusoh, A., Cheng, W. H., Low, W. M., Nora’aini, A., and Megat Mohd Noor, M. J. (2005). Study on the Removal of Iron and Manganese in Groundwater by Granular Activated Carbon. *Desalination*.182 (1-3), 347–353.

Khater EM Ashraf, (2006). Radiation Detection Methods, in: Nollet, L. and Poschl, M., Concentration of Radionuclides in Food and the environment: Prevention and Human Health. Marcel Dekker Inc., New York

Kinniburgh, D. G., Jackson, M. L., & Syers, J. K. (1976). Adsorption of alkaline earth, transition, and heavy metal cations by hydrous oxide gels of iron and aluminum. *Soil Science Society of America Journal*, 40(5), 796-799.

Kriš J., Dubová V (2005). Trends in Economical Treatment of Water. In: Proceedings of the New Trends in Water Management, Trenčín, ISBN 80-227-2251-0, pp. 20-25.

Kpeglo D. O., Mantero J., Darko E. O., Emi-Reynolds G., Akaho E. H. K., Faanu A., and Garcia-Tenorio R., (2014). "Radiological exposure assessment from soil, underground and surface water in communities along the coast of a shallow water offshore oilfield in Ghana." *Radiation Protection Dosimetry* 163(3), 341-352.

Kumar N. S., Reddy A. S., Boddu V. M., & Krishnaiah A. (2009) Development of chitosan-alginate based biosorbent for the removal of p-chlorophenol from aqueous medium, *Toxicological & Environmental Chemistry*, 91(6), 1035-1054.

Kundu S., Pal A., Mandal M., Ghosh K.S., Panigrahi S. and Pal T., (2012) Hardened Paste of Portland Cement—A New Low-Cost Adsorbent for the Removal of Arsenic from Water, *Journal of Environmental Science and Health*, Part A, 39(1), 185-202.

Lal, Devendra, and B. Peters (1967). "Cosmic ray produced radioactivity on the earth." Kosmische Strahlung II/Cosmic Rays II. *Springer Berlin Heidelberg*, 551-612.

Langmuir I. (1918). The adsorption of gases on plane surface of glass, mica and platinum. *Journal of American Chemical Society*, 40, 1361-1403.

Ma X. and Zhou,J., (2012). Adsorption of Heavy Metal Ions Using Hierarchical $CaCO_3$ – Maltose Meso/Macroporous Hybrid Materials: Adsorption Isotherms and Kinetic Studies. *Journal of Hazadous Materials*, 209-210, 467- 477.

Mahmoud D.K., Mohd S.M.A., Karim W.A.W.A. (2012). Langmuir model application on solid-liquid adsorption using agricultural wastes: *Journal of Purity, Utility Reaction and Environment*, 1(4), 170-199.

Mook W. (2000). "Chemistry of carbonic acid in water", pp. 143–165 in Environmental Isotopes in the Hydrological Cycle: Principles and Applications. INEA/UNESCO: Paris

Nor A., Hamidi A.A., Mohd Nordin A., Pulau P.P., and Nibong T., (2016). "Potential of high quality limestone as adsorbent for iron and manganese removal in groundwater." *Jurnal Teknologi*, 78(4), 77-82.

Nor Azliza, Hamidi Abdul Aziz, and Mohd Nordin Adlan. (2015).Iron and Manganese Removal from Groundwater Using High Quality Limestone." *Applied Mechanics and Materials*. Vol. 802. Trans Tech Publications.

Nouri, L., Ghodbane, I., Hamdaoui, O., and Chiha, M. (2007). Batch sorption dynamics and equilibrium for the removal of cadmium ions from aqueous phase using wheat bran. *Journal of Hazardous Materials*, *149*(1), 115-125.

Peköz R., Karen J., and Davide D., (2012). "Adsorption of dichlorobenzene on Au and Pt stepped surfaces using van der Waals density functional theory." *The Journal of Physical Chemistry C* 116(38), 20409-20416.

Postawa A., Hayes C., Criscuoli A., Macedonio F., Angelakis A. N, Rose J. B., Maier A., McAvoy D. C. (2013). *Best Practice Guide on the Control of Iron and Manganese in Water Supply*. London, IWA Publishing,

Sharma S.K., Greetham M.R., and. Schippers J. C., (1999) "Adsorption of iron (II) onto filter media." *Journal of Water Supply: Research and Technology-Aqua* 48(3), 84-91.

Shela Osborne N., (2000). "Management of shared river basins: the case of the Zambezi River." *Water Policy* 2(1), 65-81.

Teunissen, K., Abrahamse, A., Leijssen, H., Rietveld, L., and van Dijk, H.: (2008). Removal of both dissolved and particulate iron from groundwater, Drink. *Water Eng. Sci. Discuss.*, 1, 87-115.

Thomas J.W., and Crittenden B., (1998). *Adsorption Technology and Design*. Great Britain. Butterworth-Heinemann.

Tran H. N., You S-J., Hosseini-Bandegharaei A., Chao H-P., (2017). Mistakes and inconsistencies regarding adsorption of contaminants from aqueous solutions: A critical review. *Water Research*, 120, 88-116.

United Nations Scientific Committee on the Effects of Atomic Radiation, and B. Annex. (2000). "Exposures from natural radiation sources." New York, United Nation.

Wang Y., Saraya S., and Timothy G.T., (2013). "Ferrous iron removal by limestone and crushed concrete in dynamic flow columns." *Journal of Environmental Management*, 124, 165-171.

World Health Organization & International Programme on Chemical Safety. (1996). Guidelines for drinking-water quality. Vol. 2, Health criteria and other supporting information, 2nd Ed. Geneva: World Health Organization. Available at: http://www.who.int/iris/handle/1

APPENDIX A

A1 SAMPLE COMPOSITION RESULTS

ACCELERATOR RESEARCH CENTRE

National Nuclear Research Institute, Ghana Atomic Energy Commission, P. O. Box, 80, Legon.

In case of reply the number and
Date of this letter should be quoted
Telephone: 0302400807
Fax:233302400807
Our Ref: ARC/IBA/1/Vol.I/2
Your Ref. No.....

18TH April, 2017

SAMPLE ANALYSIS REPORT
Client name: Thandiwe Phiri
Supervisor: Dr. S.K. Dampare, SNAS

Ekloo1b

Compound	Wt (%)	Error
SiO_2	661555	3.34
K_2O	41317	0.85
CaO	235596	0.42
TiO_2	5412	2.6
Cr_2O_3	177	37.02
MnO	662	12.97
Fe_2O_3	52600	1.06

Ekloo1b

Element	ppm	Error
Si	316230.5	3.34
K	33007.8	0.85
Ca	163795.1	0.42
Ti	2934.5	2.61
Cr	101	37.1
Mn	454.5	12.96
Fe	33799.6	1.06

Ekl001f

Compound	Wt (%)	Error
SiO_2	513291	3.61
K_2O	24634	0.98
CaO	441448	0.32
TiO_2	2655	3.45
MnO	891	10.51
Fe_2O_3	16242	1.79

Ekl001f

Element	ppm	Error
Si	218901.3	3.81
K	21534.9	1.11
Ca	342331.6	0.32
Ti	2084.1	3.73
Mn	729.3	14.37
Fe	14260.5	1.9

Eklr02

Compound	Wt(%)	Error
SiO_2	196829	6.47
SO_3	470	24.75
K_2O	5167	2.71
CaO	785247	0.3
TiO_2	1159	11.2
MnO	682	13.45
Fe_2O_3	7542	3.39
ZnO	159	75.01

Eklr02

Element	ppm	Error
Si	91911.4	6.88
S	189.7	61.93
K	4288.8	2.69
Ca	561398.1	0.29
Ti	695	7.86
Mn	528.2	14.6
Fe	5276.8	3.37
Zn	127.6	67.62

Comment: Results presented are based on samples as submitted by client

Sign of Analyst

Sign Manager, ARC.

A2: Calculation of Percentage Composition

Results of the components present in the rock samples after being tested with the linear accelerator at Ghana atomic energy commission GAEC were given. The front and back sides of the samples were analysed this is due to one side being 0.1 cm thick and the other being 1cm thick with each side having different ratios of the components present, an average of each element was calculated and recorded to obtain the mean value of the element in the samples.

The results were presented in ppm (parts per million) and conversion of 1 ppm to percentage is as follows;

$1\text{ppm} = \frac{1}{1000000} = 0.000001 = 1\times10^{-6}$

$1\times10^{-6} \times 100\%$

1 ppm = 0.0001%

This formula was used to calculate the individual percentages of each of the elements and compounds as follows;

Silicon Percentage

EKLD01F

218901 × 0.0001 %

= 21.89 %

EKLD01B

316230.5 × 0.0001%

= 31.62 %

EKLR02

91911.4 × 0.0001 %

= 9.19 %

Appendix B Activity Concentrations of Samples

- **B1 Sample EKLDO1 grain size 1(2000-6350)**

	Radionuclide	Energy(Kev)	Net Area	Net error	Counting Time	Mass	Activity
U-238 series	Pb-210	46.5	542	8.67E+01	36000	0.556	48.15208292
	Th-234	63.29	1950	1.60E+02	36000	0.556	89.96615476
	Pb-214	295.224	10187.6	1.29E+02	36000	0.556	82.04062992
		351.932	17680	1.57E+02	36000	0.556	80.90438078
		241.997		0.00E+00	36000	0.556	
	Bi-214	609.312	12938.6	1.27E+02	36000	0.556	81.88628331
		1120.287	2806.64	6.90E+01	36000	0.556	83.75634401
		1764.494	2371.27	5.31E+01	36000	0.556	85.53166419
Th-232 series	Pb-212	238.632	746.4	8.21E+01	36000	0.556	2.063398146
	Tl-208	583.191	972.87	6.37E+01	36000	0.556	9.144652313
		510.77		0.00E+00	36000	0.556	
		860.564		0.00E+00	36000	0.556	
	Ac-228	338.32	571.32	7.25E+01	36000	0.556	8.420411126
		911.204	652.27	5.22E+01	36000	0.556	8.842784272
		968.971	255.99	4.63E+01	36000	0.556	5.907101239
	Ra-224	240.986		0.00E+00	36000	0.556	
	Bi-212	727.33	183.38	1.11E+01	36000	0.556	
k-series	K-40	1460.83	4823	7.62E+01	36000	0.556	220.41

- **B2 EKLR02 Sample Size 1(2000-6350)**

	Radionuclide	Energy(Kev)	Net Area	Net error	Counting Time	Mass	Activity
U-238 series	Pb-210	46.5	0	0.00E+00	36000	0.578	
	Th-234	63.29	0	0.00E+00	36000	0.578	
	Pb-214	295.224	1167.47	5.37E+01	36000	0.578	9.043775733
		351.932	2221.22	8.26E+01	36000	0.578	9.777510837
		241.997		0.00E+00	36000	0.578	
	Bi-214	609.312	0	0.00E+00	36000	0.578	
		1120.287	358.07	4.88E+01	36000	0.578	10.27888225
		1764.494	337.7	2.28E+01	36000	0.578	11.71720232
Th-232 series	Pb-212	238.632	8787.75	1.41E+02	36000	0.578	23.36878063
	Tl-208	583.191	2556.28	7.29E+01	36000	0.578	23.11360897
		510.77		0.00E+00	36000	0.578	
		860.564		0.00E+00	36000	0.578	
	Ac-228	338.32	1636.8	7.81E+01	36000	0.578	23.20579431
		911.204	1779.94	6.23E+01	36000	0.578	23.21207375
		968.971	934.26	5.61E+01	36000	0.578	20.73796428
	Ra-224	240.986		0.00E+00	36000	0.578	
	Bi-212	727.33		0.00E+00	36000	0.578	
k-series	K-40	1460.83	17553.49	1.35E+02	36000	0.578	211.9

- **B3 Sample EKLDO1 grain size 3 (500-1000)**

	Radionuclide	Energy(Kev)	Net Area	Net error	Counting Time	Mass	Activity
U-238 series	Pb-210	46.5	857.63	9.43E+01	36000	0.63	67.24345166
	Th-234	63.29	1512.08	1.06E+02	36000	0.63	61.56778913
	Pb-214	295.224	9717	1.36E+02	36000	0.63	69.05951856
		351.932	17086.39	1.49E+02	36000	0.63	69.00401083
		241.997		0.00E+00	36000	0.63	
	Bi-214	609.312	12523.48	1.21E+02	36000	0.63	69.94926276
		1120.287	2696.04	6.50E+01	36000	0.63	71.00543216
		1764.494	2279.38	5.13E+01	36000	0.63	72.55993596
Th-232 series	Pb-212	238.632	746.4	3096.77	8.76E+01	0.63	7.555350186
	Tl-208	583.191	972.87	937.35	6.39E+01	0.63	7.775859634
		510.77		0.00E+00	36000	0.63	
		860.564		0.00E+00	36000	0.63	
	Ac-228	338.32	1385.58	2.12E+02	36000	0.63	18.02269433
		911.204	714.7	5.26E+01	36000	0.63	8.551054019
		968.971	2734.79	6.21E+01	36000	0.63	55.69415755
	Ra-224	240.986		0.00E+00	36000	0.63	
	Bi-212	727.33	183.38	1.11E+01	36000	0.63	
k-series	K-40	1460.83	4904.51	7.70E+01	36000	0.63	197.8080284

- **B4 EKLR02 sample size3 (500-1000)**

	Radionuclide	Energy(Kev)	Net Area	Net error	Counting Time	Mass	Activity
U-238 series	Pb-210	46.5	0	0.00E+00	36000	0.674	0
	Th-234	63.29	327.14	7.47E+01	36000	0.674	12.45068059
	Pb-214	295.224	1211.24	5.84E+01	36000	0.674	8.046410799
		351.932	2681.77	8.90E+01	36000	0.674	10.12339542
		241.997		0.00E+00	36000	0.674	
	Bi-214	609.312	2064.27	7.27E+01	36000	0.674	10.77718329
		1120.287	480.92	5.11E+01	36000	0.674	11.83910126
		1764.494	404.5	2.58E+01	36000	0.674	12.03592122
Th-232 series	Pb-212	238.632	9298.86	1.47E+02	36000	0.674	21.20586584
	Tl-208	583.191	2388.58	6.45E+01	36000	0.674	18.52111264
		510.77		0.00E+00	36000	0.674	
		860.564		0.00E+00	36000	0.674	
	Ac-228	338.32	1755.51	8.34E+01	36000	0.674	21.34381616
		911.204	1948.79	6.33E+01	36000	0.674	21.79423168
		968.971	761.88	5.52E+01	36000	0.674	14.5028342
	Ra-224	240.986			36000	0.674	
	Bi-212	727.33	612	2.27E+02	36000	0.674	
k-series	K-40	1460.83	18883.11	5.34E+01	36000	0.674	265.1

Appendix C Column Experiment

C1 Initial UV spectrophotometer Absorbance Readings

Sample ID	Experimental Run		
	1	2	3
AS01	0.0006	0.0004	0.0008
AS02	0.0009	0.0007	0.0007
AS03	0.0007	0.0005	0.0007
AS04	0.0004	0.0004	0.0004
AS05	0.0014	0.0016	0.0013
AS06	0.0012	0.0012	0.0011
AS07	0.0119	0.0117	0.0117
AS08	0.0003	0.0003	0.0004
AS09	0.0001	0.0002	0.0002
AS10	0.011	0.0010	0.0013
AS11BH	0.0017	0.0017	0.0015
AS11BHT	0.0002	0.0003	0.0003
AS12	0.0128	0.0126	0.0129
AS13	0.0490	0.0510	0.0495

C2 Final Absorbance Readings

Samples ID	Experimental Run		
	1	**2**	**3**
AS01	0.0003	0.0003	0.001
AS02	0.0005	0.0004	0.0005
AS03	0.0003	0.0003	0.0001
AS04	0.0001	0.0002	0.0003
AS05	0.0009	0.0008	0.0005
AS06	0.0001	0.0001	0.0003
AS07	0.0001	0.0002	0.0002
AS08	0.0002	0.0001	0.0001
AS09	0.00005	0.00006	0.00005
AS10	0.0001	0.0004	0.005
AS11BH	0.0002	0.0004	0.0009
AS11BHT	0.00005	0.00005	0.00006
AS12	0.0005	0.0006	0.0008
AS13	0.0007	0.0009	0.0009

C3 Initial Iron Concentrations of Samples Collected

Sample ID	Experimental Trial			Average
	1	2	3	
AS01	0.2342	0.2523	0.2162	0.2342
AS02	0.2613	0.2432	0.2432	0.2492
AS03	0.2432	0.2252	0.2432	0.2372
AS04	0.2162	0.2162	0.2072	0.2132
AS05	0.3063	0.3243	0.2973	0.3093
AS06	0.2883	0.2883	0.2793	0.2853
AS07	1.2523	1.2342	1.2342	1.2402
AS08	0.2072	0.2072	0.2162	0.2312
AS09	0.1892	0.1982	0.1982	0.1952
AS10	0.2793	0.2703	0.2973	0.2823
AS11BH	0.3333	0.3333	0.3153	0.3273
AS11BHT	4.5946	4.7748	4.6397	4.6695
AS12	0.1982	0.2072	0.2072	0.2072
AS13	1.3333	1.3153	1.3423	1.3303

C4 Final Iron Concentration after Analysis Using the Limestone Technique

Sample ID	Experimental Trial			Average
	1	2	3	
AS01	0.2072	0.2072	0.1892	0.2012
AS02	0.2253	0.2162	0.2253	0.2227
AS03	0.2072	0.2072	0.1892	0.2228
AS04	0.1892	0.1982	0.2072	0.1982
AS05	0.2613	0.2523	0.2252	0.2463
AS06	0.1892	0.1892	0.2072	0.1952
AS07	0.1892	0.1982	0.1982	0.1952
AS08	0.1982	0.1892	0.1892	0.1922
AS09	0.1847	0.1856	0.1847	0.1850
AS10	0.2432	0.2162	0.2252	0.2282
AS11BH	0.3604	0.2162	0.2613	0.2793
AS11BHT	0.2432	0.2613	0.2613	0.2553
AS12	0.1847	0.1347	0.1856	0.1850
AS13	0.1847	0.1856	0.2523	0.2075